MASS. INST. OF TECHNOLOGY
JUN 11 1959
LIBRARY

Later Refraction Arrivals in Layered Liquids

by

Robert Alden Phinney

Submitted in partial fulfillment of the requirements for the degree of Bachelor of Science and Master of Science in Geology and Geophysics at the MASSACHUSETTS INSTITUTE OF TECHNOLOGY

June, 1959

Signature of Author .....
Robert Alden Phinney

Certified by .....
Thesis Supervisor

Head of Department .....
R. R. Shrock

Abstract

Tolstoy's theory on the dispersive properties of layered acoustic waveguides is applied to problems connected with the detection of so-called later refraction arrivals in refraction prospecting. His theory of antiresonant lattices is applied in a number of cases to develop a simple technique for estimating the dispersion curves and important later-arrival frequencies. Two cases pertinent to shallow water problems have been worked out in this way, and the results compared with curves calculated on an IBM 704 digital computer. It is seen that the simple method gives predictions which are of fairly broad applicability, as well as providing additional information about the modes of propagation not apparent in the exact solution.

In addition to the lattice method, other well-known spectral considerations are brought to bear on the question of the actual time variation of refraction arrivals. Certain features are predicted whose nature must be understood in order for a refraction record to be properly interpreted. The effects of time scaling, thickness of layers, and velocity contrast on refraction arrivals are considered. Also discussed are problems encountered in field practice when variables such as hydrophone depth, filtering, and recording speed must be optimized to obtain later refraction arrivals. Suggestions have been made for investigation of perturbations in the layer thicknesses and predictions made of their effect on refraction arrivals.

Table of Contents

Introduction	5
Chapter I Review of the pertinent theory	8
Chapter II Application to the determination of refracted arrivals	24
Chapter III Discussion and results	32
Chapter IV Considerations affecting the detection and interpretation of refracted signals	42
Appendix I Table of symbols	61
Appendix II Outline of the Buzzards Bay refraction study	62
Appendix III Tabulated results from the 704: Phase and group velocity for Model Ia Graphs of group velocity	 66 70
Appendix IV 704 program in SAP language	74
Bibliography	82

Illustrations

Figures 1 - 10	20
Figures 11 - 18	29
Plates 1 - 4	38
Plates 5 - 8	70

Acknowledgements

The author wishes to acknowledge the generous help of Mr. Norman Ness in programming for the IBM 704 computer. He is deeply indebted to his wife, Beth, for doing most of the clerical work connected with preparing this thesis.

This work was done in part at the M. I. T. Computation Center, Cambridge, Massachusetts.

Introduction

In the application of seismic refraction methods to shallow water situations, the geometry present often makes it impossible to observe first arrivals from layers overlying the basement. When first arrivals are observed, it is common for the slope and intercept of the appropriate line in the travel-time plane to be intolerably sensitive to uncertainties in the data. Consequently an effort is always made to pick intermediate layer refraction arrivals which occur after the first arrivals from the basement. Because of difficulties attendant on distinguishing these signals on the disturbed trace from random fluctuations in background level, predictions based on later arrivals are treated with some skepticism.

As we shall see in this paper, later arrivals may display features which, if not properly understood, may lead to wrong conclusions. At the same time, however, the occurrence of these features may make possible positive identification of later arrivals.

The shallow water environments to which this discussion is applicable will generate different problems in later arrivals picking. Typical inshore areas, such as Buzzards Bay, Massachusetts, are best described as plane acoustic waveguides. Consequently each refraction arrival contributes an essentially undamped wave train, and the "noise"

background for later arrival picking is a superposition of several such wave trains. In such a case we may use our first order knowledge of the geology to help distinguish arrivals from this noise, using the criteria to be discussed in this paper. Typical continental shelf refraction records tend to be less obscured by "noise" from the normal modes than they are by hydrophone and instrument noise, due to the higher sensitivity and amplification needed to detect the information.

A description of later arrivals is here based on the liquid layer theory of Pekeris, and the calculations are performed according to the scheme of Tolstoy. It is assumed that the reader is familiar with the theory of normal mode propagation as discussed in GSA Memoir 27 (1958)[15] and Ewing, Jardetzky, and Press (1957)[7*]. The main features of Tolstoy's work will be outlined and discussed without proof in thispaper, since later refraction arrivals can be best described by this rather different approach. It is also assumed that the reader has some acquaintance with the details of the seismic refraction technique at sea. Instrumentation, records, and calculations are covered in the series of papers "Geophysical Investigations in the Emerged and Submerged Atlantic Coastal Plain"[6,9,10] and in GSA Memoir 27.

Chapters I and II deal with Tolstoy's work concerning dispersion in layered acoustic waveguides. It is shown how

---

* Superscripts refer to numbered references in the bibliography.

the lattice approximations can be applied to two different models to deduce the character of the dispersion without prolonged calculation. For these cases predictions about the later refraction arrivals are tabulated for comparison with results obtained by a digital computer. In Chapter III dispersion and group velocity curves for twelve different cases as calculated on the IBM 704 digital computer are presented. Later arrivals deduced from these curves are compared with prediction made by application of the lattice approximations. The curves used to generate the lattices are discussed in terms of the geometrical factors which affect refraction arrivals from finite thickness layers. The structure of the 704 program is detailed in an appendix.

The actual appearance of later arrivals is mentioned qualitatively in Chapter IV. Criteria are developed for intelligent picking of records. The dispersion and group velocity curves illustrate several points. Also considered is the question of attenuation of the refracted wave packets. Various deviations of the geometry from that of a plan wave-guide introduce losses by radiation into the basement and by smearing of the energy into poorly defined wave packets by transitions between modes. Ordinary volume scattering and attenuation also selectively reduce the energy of refraction arrivals. Since higher modes are generally more susceptible to these mechanisms, the importance of low mode group velocity maxima in determining refracted signals is emphasized.

Chapter I

Review of the Theory

The theory of sound propagation in stratified liquid waveguides has been enunciated by Pekeris[15], Jardetzky[11], Tolstoy[20-24], Ewing & Press[8], and others; it is not the purpose of this paper to present or review all of this theory, except as it touches on the problem at hand.

Pekeris[15] has shown that the contribution to a steady state acoustic potential is composed of two parts. A branch-line integral represents the continuous spectrum, giving rise to the transient pulse observed in seismic refraction as the "refracted arrival." Jardetzky[11] proved that only one branch line integral exists for an n-layered problem, and that it was identified with the branch point

$$k = \alpha_n \qquad (1)$$

The remainder of the signal is generated by a nonorthogonal discrete set of modes, which arise mathematically from pole contributions to a contour integral in the complex k-plane. These "normal modes" constitute the principal signal observed at long ranges, since they are caused physically by constructive interference of totally reflected plane waves in the finite part of the waveguide. The normal modes are dispersive. The horizontal phase velocity, c, is frequency dependent; hence it is appropriate to form the group velocity:

$$U = \frac{d\omega}{dk} = c + k\frac{dc}{dk} = \frac{c^2}{c + \omega\frac{dc}{d\omega}} \qquad (2)$$

which defines the velocity of a wave packet with central

frequency ω in the waveguide. Biot[2] has shown that the group velocity is also defined for a single frequency source (under liberal restrictions) as the rate of energy transport in the waveguide.

The characteristic equation which defines the dispersion of the normal modes can be obtained in straightforward manner by application of the boundary conditions to eigenfunctions of the proper form and setting the secular determinant equal to zero. For each value of c within a certain range, there will, in general, be infinitely many solutions, ω_m, corresponding to the modes m = 1,2,3,..... Inversely, for each value of ω, there will be only a finite number of c_m which solve the period equation. This is illustrated in figures 1 and 2, where typical dispersion curves are displayed in the ω-c plane and the k-ω plane.

When the sound source is a transient, it is necessary to perform an appropriate Fourier synthesis of the steady state solutions. If the source dependence is

$$f(t) = \begin{cases} e^{-\lambda t} & (t>0) \\ 0 & (t<0) \end{cases} \qquad (3)$$

its Fourier transform will be

$$g(\omega) = \frac{1}{\lambda + i\omega} \qquad (4)$$

A representation of the steady state contribution from the normal modes is*

$$\varphi(\omega, r, z) = \sum_{m=1}^{\infty} \varphi_m(\omega, r, z) \qquad (5)$$

*Since we are not interested in the first arrivals from the lower half space, the branch line integral is ignored hereafter.

By Fourier synthesis then, the acoustic potential as a function of time will be given by

$$\Phi(r,z,t) = \frac{1}{2\pi} \sum_m \int_{-\infty}^{\infty} \frac{e^{i\omega t}}{\lambda + i\omega} \varphi_m(\omega, r, z)\, d\omega \quad (6)$$

At sufficiently long ranges the significant contribution to φ_m can be written

$$\varphi_m \approx \sqrt{\frac{2}{\pi k_m r}}\, \Psi_m(\omega)\, Z(z)\, e^{-ik_m r} \quad (7)$$

where $k_m(\omega)$ is an mth eigenvalue of the period equation. Hence

$$\Phi(r,z,t) = \frac{1}{2\pi} \sum_m \int_{-\infty}^{\infty} d\omega \cdot \frac{\Psi_m(\omega) Z(z)}{\lambda + i\omega} \sqrt{\frac{2}{\pi k_m r}}\, e^{i(\omega t - k_m r)} \quad (8)$$

This is evaluated by Kelvin's method of stationary phase; the contributions to the integral arise when

$$d(\omega t - k_m r) = 0 \quad (9)$$

$$\text{or } \frac{r}{t} = \frac{d\omega}{dk_m} \equiv U \qquad \text{: the group velocity.}$$

The resultant expression

$$\Phi = \frac{2}{rH} \sum_m \frac{U_m}{k_m} \left(\left| \frac{dU}{dk_m} \right| \right)^{-\frac{1}{2}} \frac{e^{i(\omega_m t - k_m r)}}{\lambda + i\omega_m} Z(z) P(k_m) \quad (10)$$

is valid only if $\frac{dU}{dk} = \frac{d^2\omega}{dk^2}$ is not near zero.

When the group velocity is stationary, a higher order approximation using the Airy integral must be employed. This second order theory predicts the existence of asymmetric wave packets in the transient response. The modulation of these wave packets is given by an envelope function computed

by Pekeris, shown in Figure 3. Corresponding to a group velocity maximum the envelope is reversed in time, giving a relatively sharp onset. The carrier frequency of an Airy wave packet is constant, and equals the frequency at the stationary value of group velocity. Higher approximations would be necessary if higher derivatives of U were equal to zero. Although these cases have not been worked out in detail, we should expect as a check that the higher the order of stationarity, the sharper would be the onset of a wave packet at a group velocity maximum.

Applying these remarks to the dispersion curve for a liquid layer overlying a liquid halfspace of greater sound velocity, we can deduce, after Pekeris, the form of the transient signal (Figure 4). If the mode shown constitutes the main part of the signal, we read this curve as follows. At $t = \frac{r}{\alpha_2}$ a small amplitude signal will appear at the cutoff frequency ω_c. Following will be a slightly dispersed train of waves corresponding to the high velocity branch of the group velocity curve. At $t = \frac{r}{\alpha_1}$ a high frequency signal (the direct arrival) will appear superimposed on the ground wave, corresponding to the high frequency limb of U. The two frequencies gradually merge into one high amplitude wave packet at the Airy phase.

Similarly, we can construct a signal from a more complicated dispersion curve, as found in a three-layered geometry (Figure 5).

In situations with more than 2 layers, the group velocity curve has complicated features of the shape sketched in Figure 5. One or more maxima may occur near velocities identified with the intermediate layers; the wave packets generated are interpreted as refraction arrivals from the top of the corresponding layers. In general, a single "later arrival" will be composited of several such maxima from many modes, all arriving more or less simultaneously. The existence of one or more maxima for some mode will depend on whether the appropriate layer is thick enough to support undamped oscillations by itself, in the right frequency range. Thus thin layers will not produce group velocity maxima in the lower modes.

Tolstoy, in a series of papers, has outlined a theory for determination of the dispersion and group velocity in multilayered liquids. It is the purpose of this paper to show how this theory can be quickly and easily brought to bear on problems encountered in seismic refraction studies. In particular, the person working with seismic refraction should know, in terms of this theory, how to optimize his technique and interpretation to get second arrivals. He should know what frequencies to expect and what modes are important. The high frequency cutoff of the receiving system may be critical in this respect, since the higher modes transmit more detailed information.

Commonly one or more layers may be masked, i.e. not

produce first-arrival information. Accordingly, proper interpretation of second-arrival information is essential to the detection of masked layers. In extreme shallow water situations with shallow bedrock, the nature and possible thickness of the intermediate sediments can then be inferred. A recent program carried out in Buzzards Bay, Massachusetts, by Elizabeth Bunce and the present author[3] presented such problems, and was the motivation for this investigation. Appendix II contains a description of this work, with emphasis put on aspects pertinent to the present paper.

* *

The period equation has been derived in a general way by Tolstoy[21], using the idea of generalized reflection coefficients.

If we consider two liquid halfspaces with a plane interface (Figure 6), the acoustic amplitude reflection coefficient for plane waves is given by

$$R_{01} = \frac{r_0 \rho_1 - r_1 \rho_0}{r_0 \rho_1 + r_1 \rho_0} \qquad (11)$$

If medium (1) is replaced by an n-layer ensemble, bounded by a half space, the quantity defined as the complex amplitude ratio of the wave reflected by the ensemble back into the (0) region and the incident wave is the generalized reflection coefficient $\mathcal{R}_{01}^{(n)}$. $\mathcal{R}$ can be obtained by summing

up the infinite series of ray paths (Figure 7), or by using a set of recursion formulas:

$$\mathcal{R}_{j,j+1}^{(n-j)} = \frac{R_{j,j+1} + \mathcal{R}_{j+1,j+2}^{(n-j-1)} e^{2i r_{j+1} h_{j+1}}}{1 + R_{j,j+1} \mathcal{R}_{j+1,j+2}^{(n-j-1)} e^{2i r_{j+1} h_{j+1}}} \qquad (12)$$

with the boundary condition:

$$\mathcal{R}_{n,n+1}^{(0)} = R_{n,n+1} \qquad (13)$$

A similar set of coefficients, the $\mathcal{R}_{j,j-1}^{(j-1)}$ refer to incident waves traveling upward in the structure.

The half-angle of phase change induced by the boundary on the reflected wave is defined by:

$$\mathcal{R}_{j,j+1}^{(n-j)} = e^{2i \chi_{j,j+1}^{(n-j)}} \qquad (14)$$

χ will be real if the conditions for total reflection hold at any interface, and will be imaginary if any ray paths penetrate the lower halfspace.

The conditions for guided waves to exist, from which we shall write down the period equation, are:[20]

1. Total reflection shall prevent energy from being propagated into the halfspaces bounding the layered structure.

2. If we consider families of guided plane waves, with the energy confined to two dimensional propagation (in the compound plate consisting of the layers), we must require that the signal measured at two points of the same depth be indistinguishable with respect to amplitude and phase.

In the situation pictured in Figure 8, then, the period equation is:

$$\mathcal{R}\uparrow \mathcal{R}\downarrow e^{2ir_ih_i} = 1 \qquad (15)$$

or:

$$\chi\uparrow + \chi\downarrow + r_ih_i = m\pi \qquad (16)$$

where $\mathcal{R}\uparrow$ is the generalized reflection coefficient for upgoing plane waves incident on the overlying region, and the other quantities are similarly defined. The integer m defines the mode number.

Appropriate specialization of Eq.16 provides a system of equations which define the eigenvalues of the problem. In terms of an n-layered structure, equation 16 reads:

$$\chi_{i,i+1}^{(n-i)} + \chi_{i,i-1}^{(i-1)} + r_ih_i = m\pi \qquad (17)$$

The recursion formula, equation 12, written in terms of the phase angles χ , is:

$$\chi_{i,i+1}^{(n-i)} = \tan^{-1}\left[\frac{r_i}{r_{i+1}}\frac{\rho_{i+1}}{\rho_i}\tan\left(r_{i+1}h_{i+1} + \chi_{i+1,i+2}^{(n-i-1)}\right)\right] \qquad (18)$$

The boundary condition, equation 13, becomes:

$$\chi_{n,n+1} = \tan^{-1}\left[\frac{r_n}{r_{n+1}'}\frac{\rho_{n+1}}{\rho_n}\right] \qquad (19)$$

where r_{n+1}' is the imaginary vertical wave number in the halfspace n + 1 , so written because total reflection is assumed at the n - (n + 1) interface. In terms of guide phase velocity c, this means:

$$--- \alpha_{n-1} < \alpha_n < c < \alpha_{n+1} \qquad (20)$$

In general we shall assume that the sound velocity in the layers increases with depth: $\alpha_j < \alpha_{j+1}$

If c lies in come other range of values, obvious changes in certain of the recursion formulas are called for.

Combining equation 17 and equation 18, the period equation, written in terms of the top layer, becomes:

$$\psi_1 = r_1 h_1 + \tan^{-1}\left[\frac{r_1}{r_2}\frac{\rho_2}{\rho_1}\tan\psi_2\right] = m\pi \qquad (21)$$

where:

$$\begin{aligned} \psi_2 &= r_2 h_2 + \tan^{-1}\left[\frac{r_2}{r_3}\frac{\rho_3}{\rho_2}\tan\psi_3\right] \\ &\vdots \\ \psi_n &= r_n h_n + \tan^{-1}\left[\frac{r_n}{r'_{n+1}}\frac{\rho_{n+1}}{\rho_n}\right] = r_n h_n + \chi_{n,n+1} \end{aligned} \qquad (22)$$

When total reflection occurs at an interface, j - (j + 1), where j < n, obvious modifications of equation 22 must be made:

$$\begin{aligned} \psi'_{j+1} &= r'_{j+1} h_{j+1} + \tanh^{-1}\left[\frac{r'_{j+1}}{r'_{j+2}}\frac{\rho_{j+2}}{\rho_{j+1}}\tanh\psi'_{j+2}\right] \\ \psi_j &= r_j h_j + \tan^{-1}\left[\frac{r_j}{r'_{j+1}}\frac{\rho_{j+1}}{\rho_j}\tanh\psi'_{j+1}\right] \\ \psi_{j-1} &= r_{j-1} h_{j-1} + \tan^{-1}\left[\frac{r_{j-1}}{r_j}\frac{\rho_j}{\rho_{j-1}}\tan\psi_j\right] \end{aligned} \qquad (23)$$

In solving the period equation, if c is used as a trial parameter, and k_m is obtained by iteration, a different modification of the set (22) is necessary for each range of c used:

$$\begin{aligned} \alpha_n &< c < \alpha_{n+1} \\ &\vdots \\ \alpha_j &< c < \alpha_{j+1} \\ &\vdots \\ \alpha_1 &< c < \alpha_2 \end{aligned} \qquad (24)$$

In the more general case when $\alpha_j \not< \alpha_{j+1}$ appropriate modification of (22) is also possible.

The foregoing mathematical scheme was programmed on an IBM 704 digital computer and used to solve several cases which are discussed in Chapter III. Further details may be obtained by consulting the appendices or reference 22.

* *

Following Tolstoy[23], we consider an n-layer system to be separated along the (j + 1)th interface (Figure 9). We can write the period equation for each separate waveguide:

$$\phi_1 = p\pi \qquad p = 1, 2, \text{----} \qquad (25a)$$

$$\varphi_{j+1} = s\pi \qquad s = 1, 2, \text{-----} \qquad (25b)$$

Each equation will then define a family of curves in the $\omega - c$ plane which governs the mode propagation for its particular waveguide. These two families of curves will intersect to form a lattice of points (Figure 10). Each lattice point represents a solution to <u>both</u> separated problems, such that the pressure is a node at the free surfaces. Hence each lattice point is also a solution to the original problem, such that the pressure is a node at the j - (j + 1) interface. These lattice points then represent the subset of solutions to the n layer problem which have nodes at the j - (j + 1) interface. We can say that the lattice points couple the frequencies of the complete waveguide to those of its components.

Since the mode number m is equal to the number of nodal planes in the mth mode of the n layer problem, it is seen that

$$m = p + s \tag{26}$$

Thus the dispersion curve for the 5th mode will pass through the lattice points (p,s) = (1,4); (2,3); (3,2); (4,1). This knowledge makes it possible to estimate the location of nodal planes for any selected values of frequency and mode number.

It can also be shown that at points of this lattice the energy tends to become largely concentrated in the (j + 1)th layer. Hence the dispersion is governed by that layer at a lattice point, and the curve $\psi_i = m\pi$ will tend to osculate to the curve $\varphi_{j+1} = s\pi$. Consequently the curve $\psi_i = m\pi$ has the form indicated in Figure 10. The effect is such, that as $c \to \alpha_{j+1} + \varepsilon$, the pressure in the (j + 1)th layer becomes very large and $\varphi_{j+1} = s\pi$ describes the dispersion for the entire waveguide.

The group velocity, U, tends to $\alpha_{j+1} - \varepsilon$ at these particular lattice points, with the result that group velocity maxima are defined. The maxima of U correspond to the horizontal inflection points of $\psi_i = m\pi$ and the minima to the vertical inflection points. Tolstoy has carried out this reasoning in considerable detail and checked it numerically with a three layer calculation for the modes m = 1, 5, and 50.

The j, j + 1 lattice then has the following relationships to the dispersion of the n-layer problem:

1. Lattice points whose indices (p,s) sum to some particular value m, lie on the mth mode dispersion curve of the n layer problem.

2. This curve (m) osculates (to a good approximation) to the curve $\varphi_{j+1} = s\pi$ at the lattice point (p,s).

3. Group velocity maxima occur for values of ω defined by the lattice. The group velocity at a maximum can be estimated by differentiation of the osculating curve $\varphi_{j+1} = s\pi$ at the lattice point.

4. Since p and s define the number of nodal surfaces for the pressure in the j layer and (n - j) layer problems, respectively, the lattice enables one to determine by inspection the distribution of nodal surfaces in the n layer problem for arbitrary values of the frequency or phase velocity.

5. Items 2 and 3 depend on the fact that $c = \alpha_{j+1} + \varepsilon$. These statements hold remarkably well for ε as large as $\frac{1}{4}\alpha_{j+1}$, and can be used to locate group velocity maxima, governed by the j + 1 layer, which propagate at velocities distinctly less than $U = \alpha_{j+1}$. Experience will enable one to regard lattice points in the low modes and at phase velocities much greater than with the proper caution.

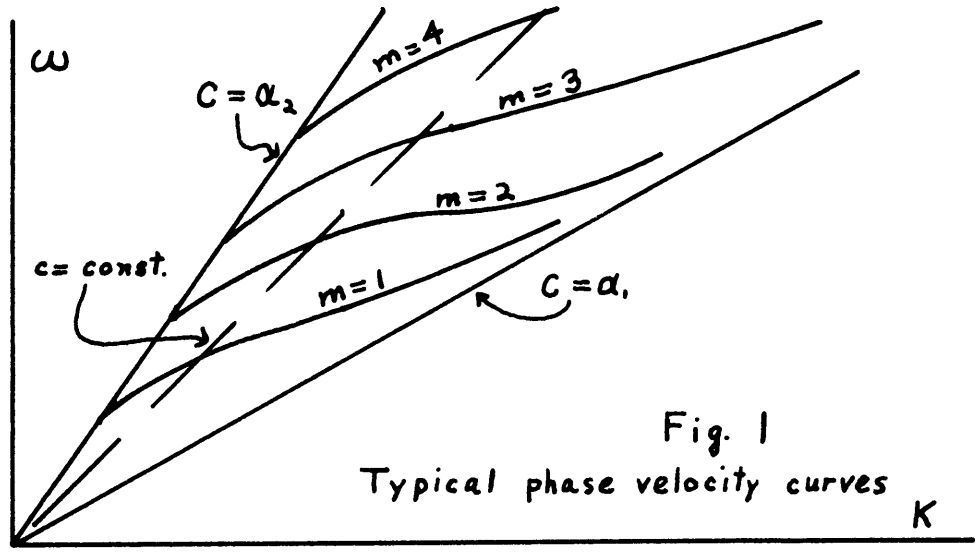

Fig. 1
Typical phase velocity curves

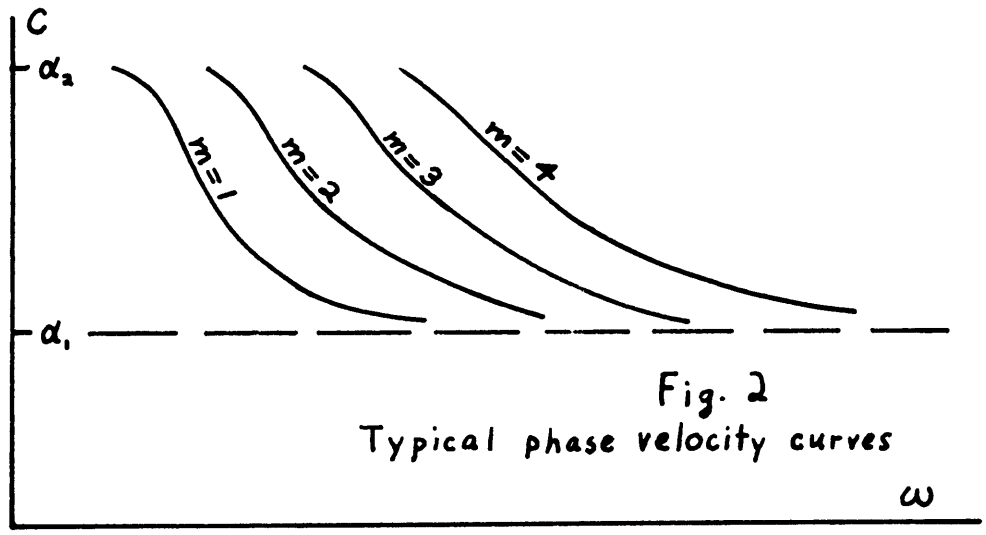

Fig. 2
Typical phase velocity curves

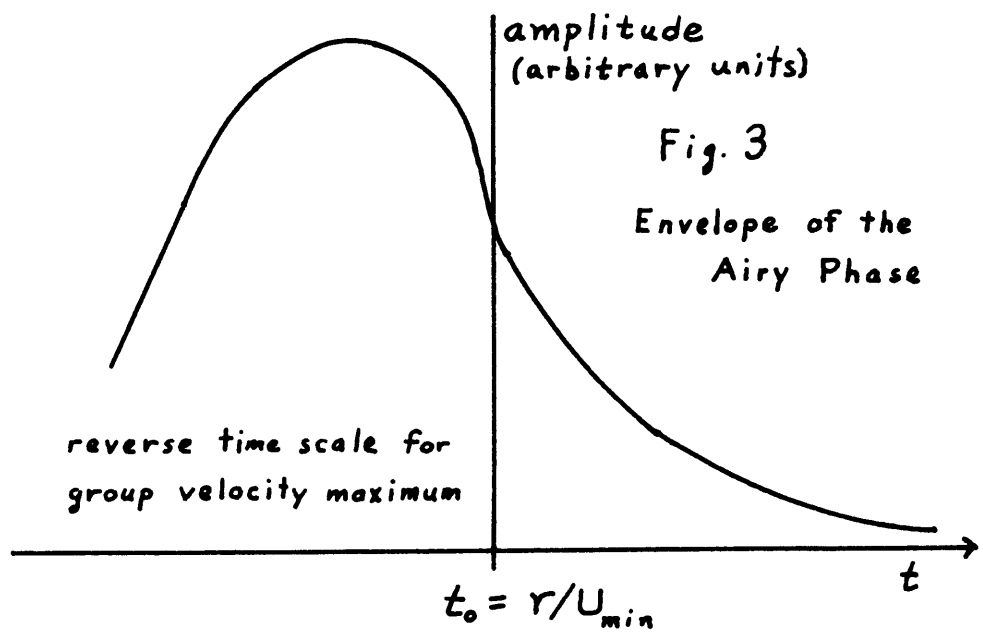

Fig. 3
Envelope of the
Airy Phase

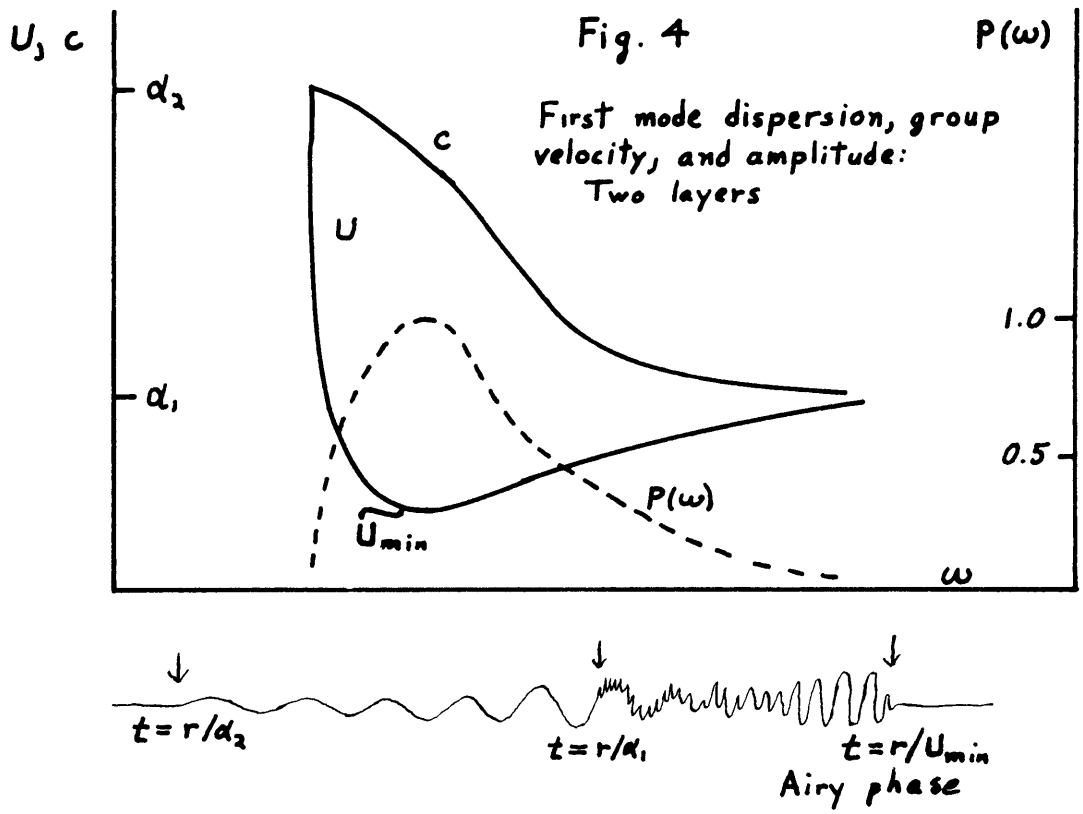

Fig. 4

First mode dispersion, group velocity, and amplitude: Two layers

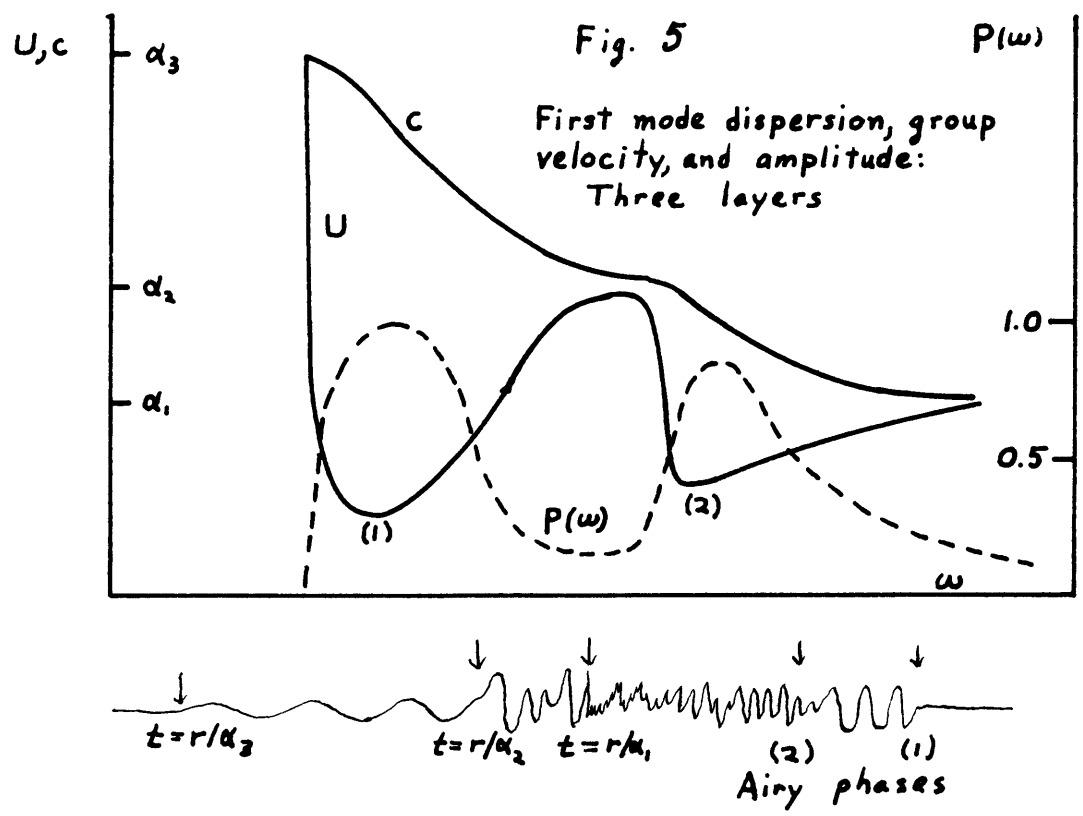

Fig. 5

First mode dispersion, group velocity, and amplitude: Three layers

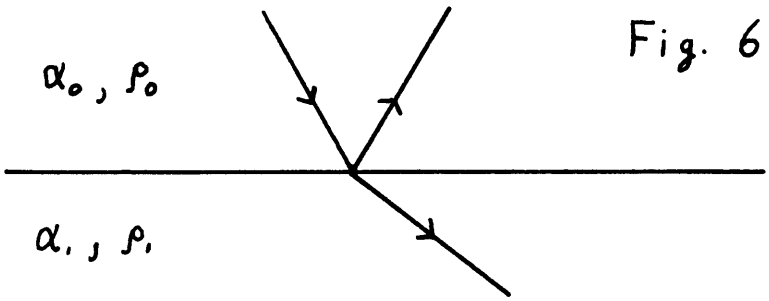

Fig. 6

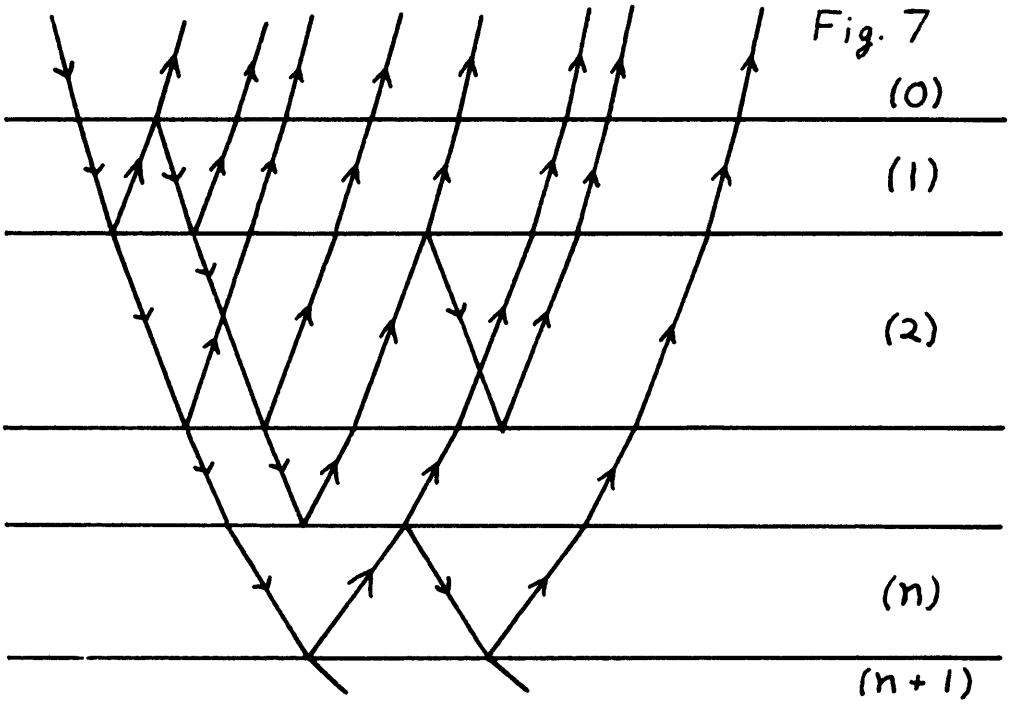

Fig. 7

Fig. 8

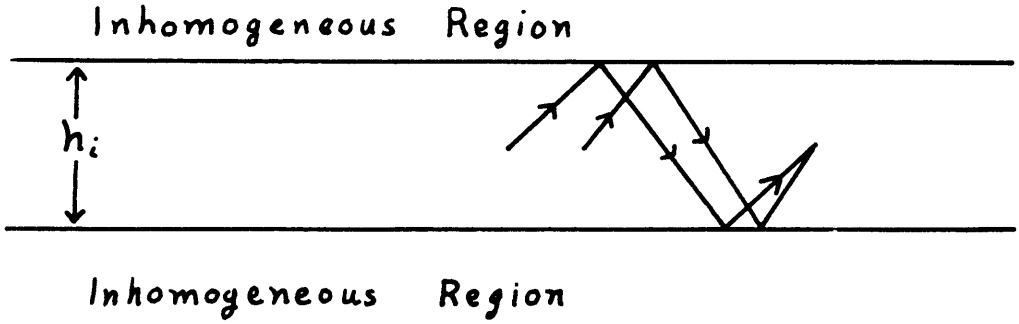

Fig. 9

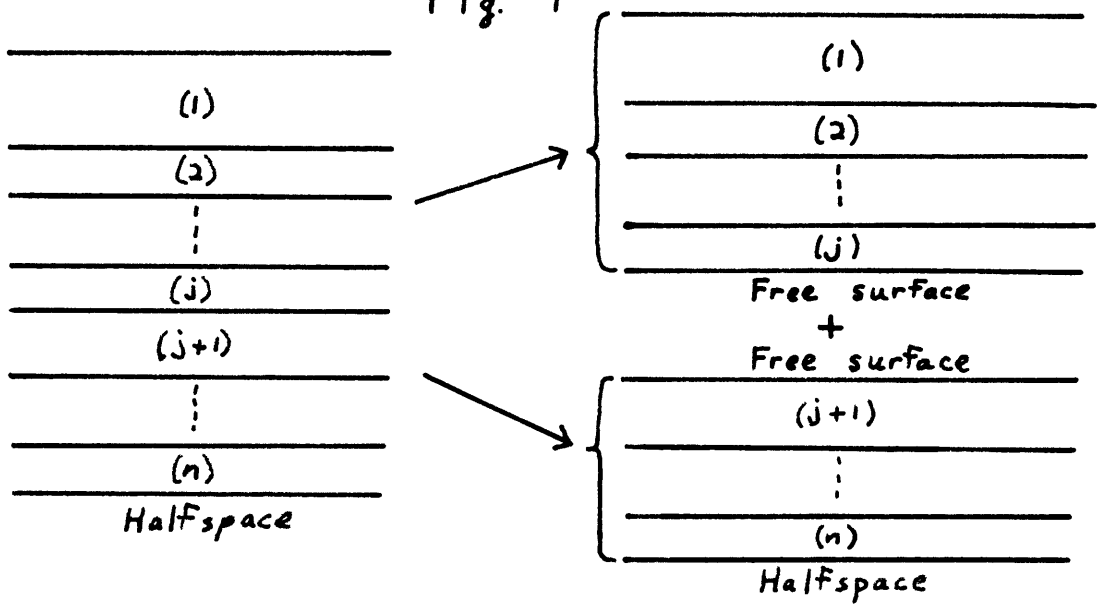
(1)
(2)
(j)
(j+1)
(n)
Halfspace
(1)
(2)
(j)
Free surface
+
Free surface
(j+1)
(n)
Halfspace

Fig. 10

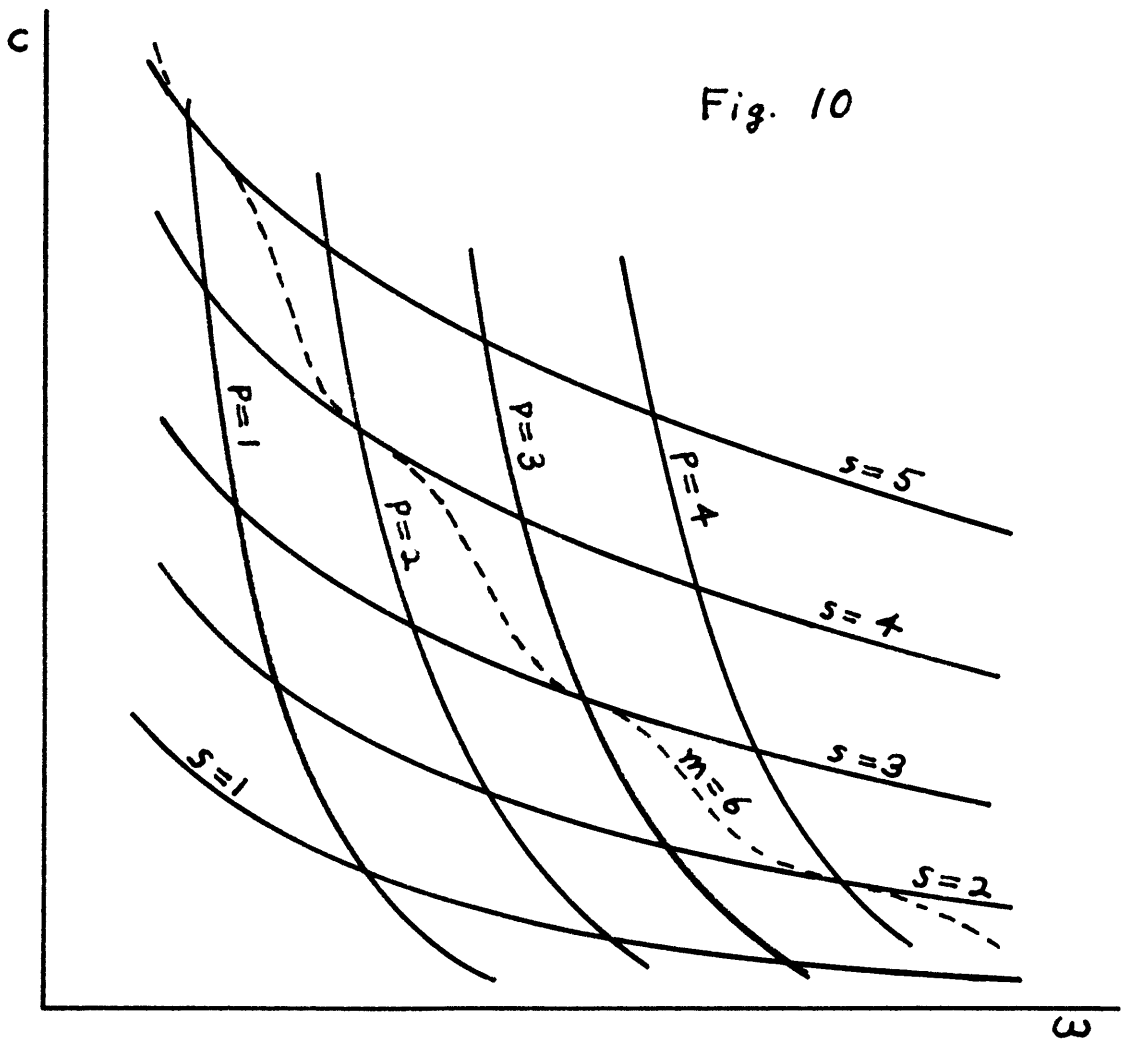
c
ω
p=1
p=2
p=3
p=4
s=5
s=4
s=3
s=2
s=1
m=6

Chapter II

We want to be able to estimate quickly, and with some accuracy, the group velocity maxima determined by intermediate layers in a structure, so that the theory will be of some use in the field and in routine reading and interpretation of records. The dispersion curve for a liquid plate bounded by free surfaces can be written explicitly: (For example, see Figure 12)

$$\omega = \frac{q_i \pi}{h_i \left(\frac{1}{\alpha_i^2} - \frac{1}{c^2}\right)^{\frac{1}{2}}} \qquad (27)$$

which can be sketched quickly, the modes forming a harmonic series in ω for all values of the argument c. As $c \to \infty$ the asymptotic difference between curves of this family is:

$$\delta = \frac{q_i \alpha_i}{2 h_i} \quad (\text{cps.}) \qquad (28)$$

We see that the spacing of eigenvalues in the spectrum is inversely proportional to the thickness of the plate, a result that is to be expected from more general considerations.

The lattice technique for estimating the dispersion curves of the complete waveguide reduces the problem to that of finding the curves for both subsets of layers $(1, 2, \text{----}, j)$, $(j+1, \text{-----}, n, n+1)$. Each of these can be solved by further reduction into subsets and using lattices to estimate the solutions. This process can be carried out as many times as desired, so that the n-layer solution can be built up of many simple curves.

It is possible to consider the n layer problem decomposed into n - 1 free plates and a plate coupled to a halfspace. The n separate problems can be used to build up solutions to the original one by lattices. They should be combined, step by step, in such a way that the final step involves the combination of waveguides along the interface j, j + 1, in whose lattice points we are interested.

In figure 11 a three layer situation is illustrated. Figure 12 shows the dispersion curves for the upper plate, calculated by equation (27). Curves for plate (2) are plotted in Figure 13, and the appropriate modification is shown by dotted lines to include the effect of coupling to the half-space, (3). Figure 14 shows the result of superimposing the two families of curves. The lattice points are indicated and dispersion curves for the 3 layer problem are sketched in. The lattice points are referred to by their indices (q_1, q_2). If the lattice were defined by more complicated ensembles, we would denote their indices by $(q_{1_{j..m}}, q_{rs..v})$.

This illustration brings out several points predicted by the theory: 1. The existence of a halfspace coupled to the waveguide causes a cutoff frequency for each mode of any subproblem coupled to the halfspace. Thus the curves for plate (2) had to be modified to account for this cutoff. For given c, the modification in f approaches $\frac{\alpha_n}{4h_n}$ as $\alpha_{n+1} > c >> \alpha_n$, and approaches zero as $c \to \alpha_1$.

2. Where the lattice points are not sufficiently dense to closely define the dispersion curve, good qualitative fit can be obtained by noting that the curve is constrained not to cross curves of either family defining the lattice except at lattice points.

3. The asymptotic behavior of the dispersion is a help in drawing curves. In this illustration, as $c \to \alpha_1$ and $c < \alpha_2$ total reflection occurs at the 1-2 interface and the dispersion is controlled mostly by the upper layer. Hence the curves m = 1 and q_1 = 1 agree asymptotically, as do m = 2 and q_1 = 2, etc.

4. The lattice point $(2,3)$ will not define, even approximately, a group velocity maximum, since c/α_2 is almost 2.6 . The remaining points drawn will define proper maxima: $(2,1)$ and $(3,1)$ are so close to $c=\alpha_2$ that we can guarantee that the corresponding maxima of U will be very close to α_2 also.

5. The first mode is always ill-defined by this method. We can estimate its cutoff frequency by halving that of the second mode; we can plot its asymptotic agreement with the curve q_1 = 1.

6. Higher modes tend to have more maxima, which are closer to $c=\alpha_2$. Figure 5 shows the possible appearance of a high mode group velocity

curve. The actual disposition of lattice points responsible for this particular mode controls the general shape of the phase velocity curve and the gross behavior of the group velocity curve as it tends from the lowest Airy minimum to slightly less than $c = \alpha_\lambda$. The inflections of the phase velocity curve as it passes through each lattice point are responsible for the detailed behavior of the group velocity, as it passes through many maxima and minima. Figure 6 shows a typical group velocity curve for some lower mode. Naturally, the number of maxima cannot exceed the mode index.

* *

A transient signal will be generated by an infinity of modes, whose higher order members have very many flat group velocity maxima, as shown in Figure 5. This makes possible the achievement of an arbitrarily sharp refracted pulse, as other considerations demand. This sharp pulse is known to be due to the discontinuity at the boundary between layers. Note that if the discontinuities were smoothed out and continuous variation of the properties substituted, the effect would be that the group velocity maxima would not have any limiting property as shown in Figure 15, but would still exist in similar quantity. This sort of problem is easily calculated by Tolstoy's equations and would be a good subject for future investigation.

To extend the plate-lattice methods to four layers, as will be necessary in the next chapter, it is most convenient to plot curves for the upper two plates and the plate-halfspace on one graph. The dispersion curve may be composited in either order:

$$(1+2)+3 \text{ or } 1+(2+3)$$

In the former case, the lattice points will give information about "refracted" signals along the 2 - 3 interface; in the latter case they will define refractions along 1 - 2. Both sets of lattice points will, however, lie on the dispersion curve itself.

Fig. 11

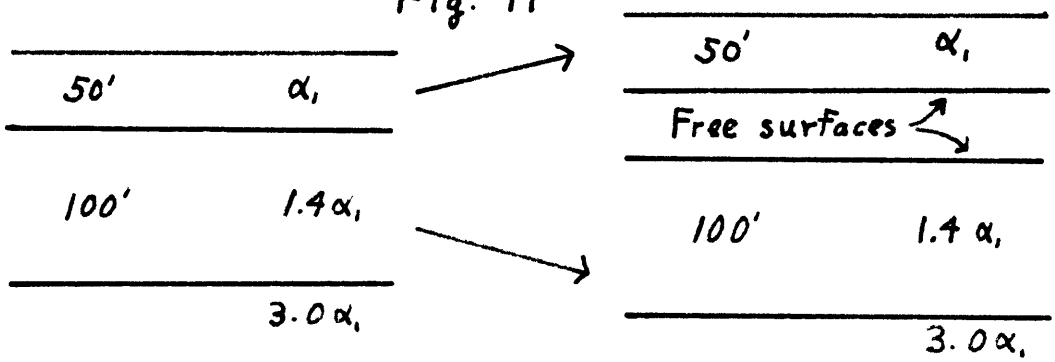

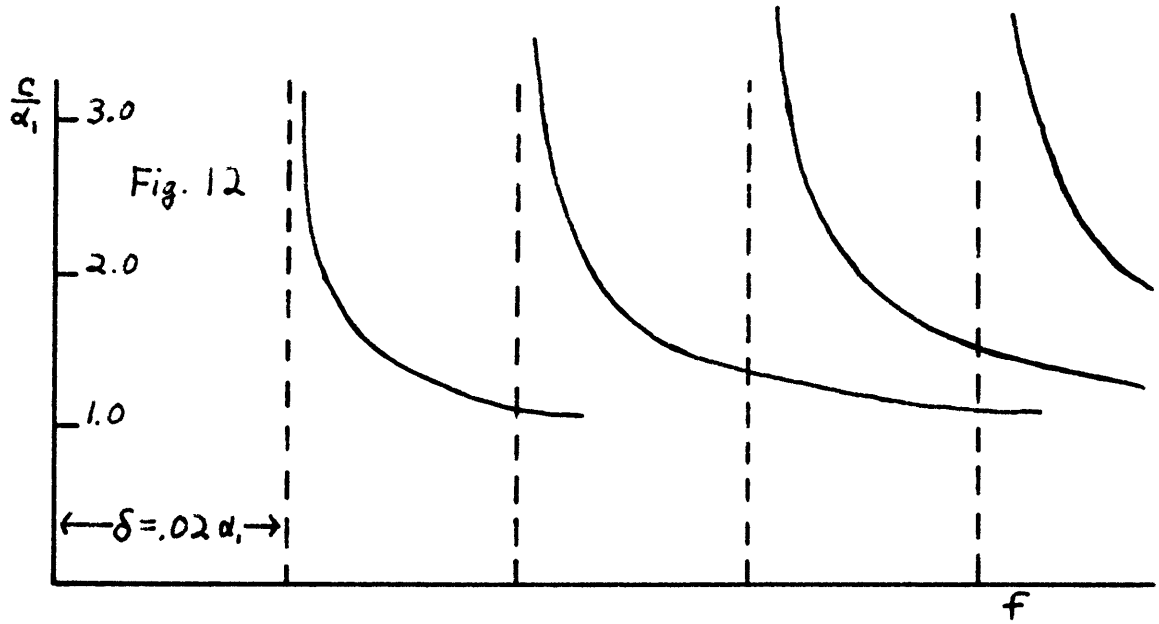

Fig. 12

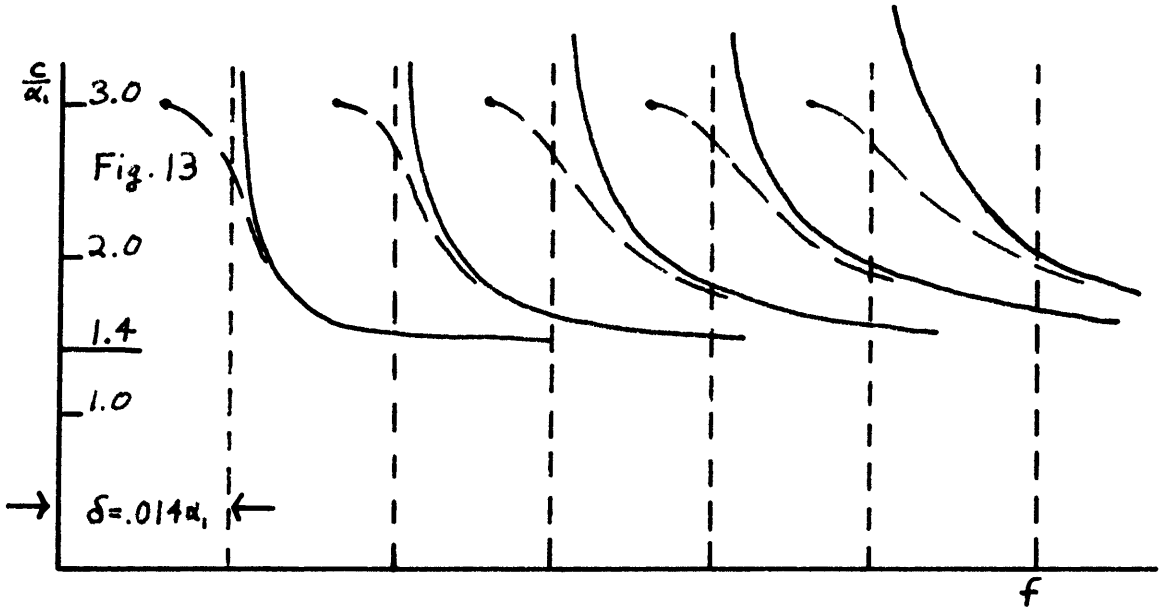

Fig. 13

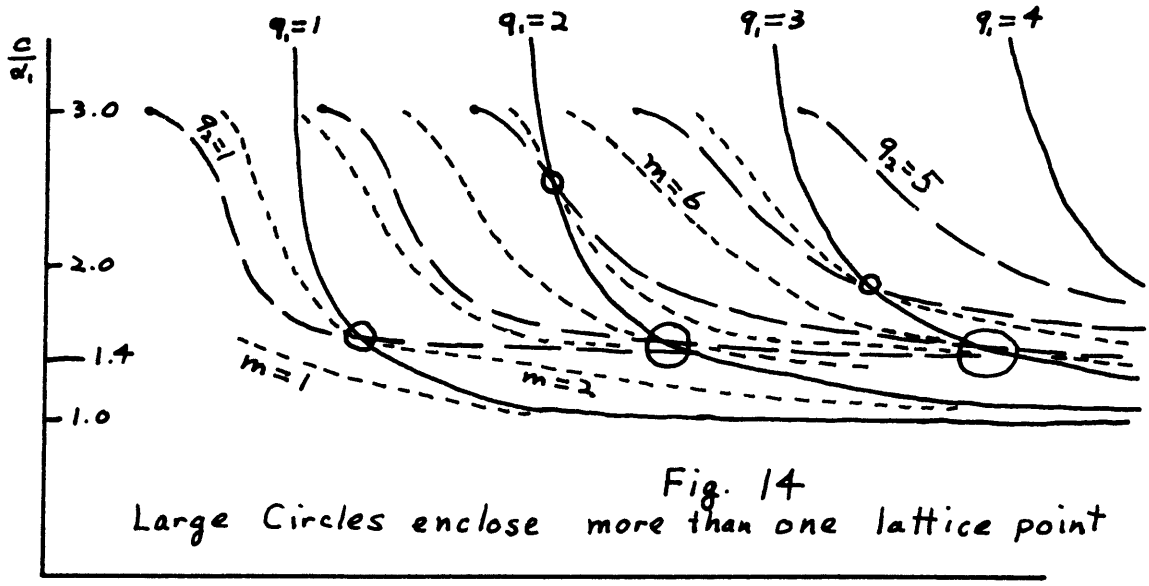

Fig. 14
Large Circles enclose more than one lattice point

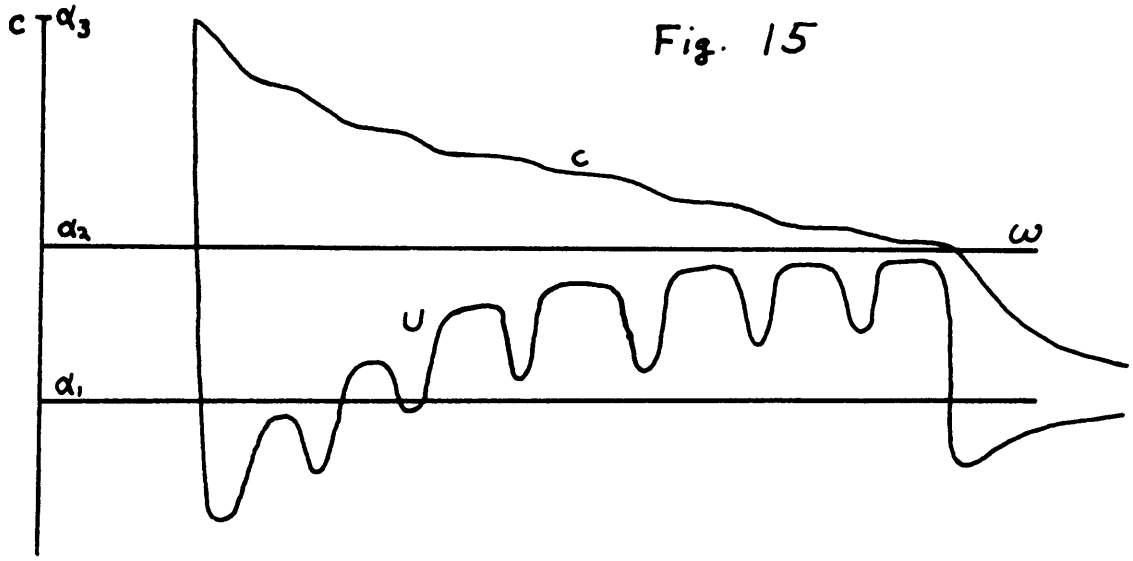

Fig. 15

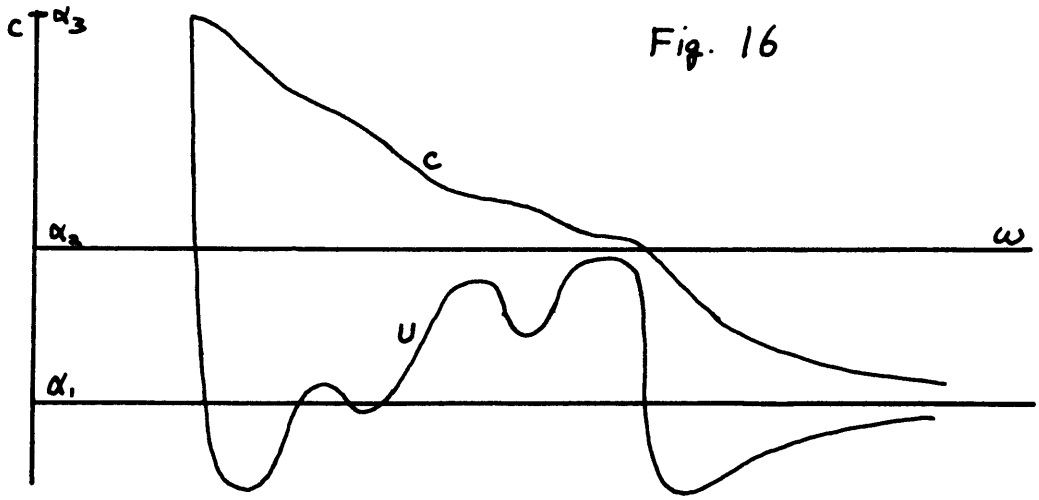

Fig. 16

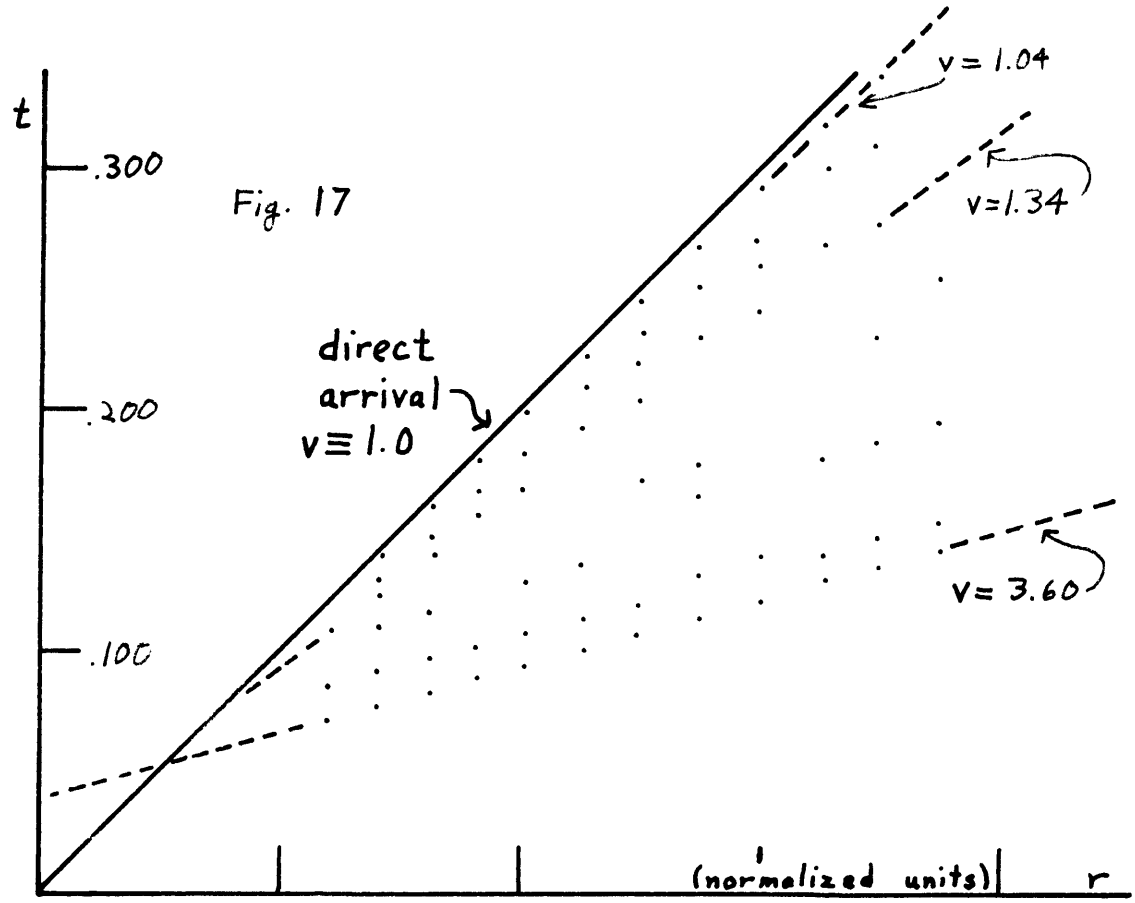
t
.300
.200
.100
Fig. 17
direct
arrival
v ≡ 1.0
v = 1.04
v=1.34
v= 3.60
(normalized units)
r

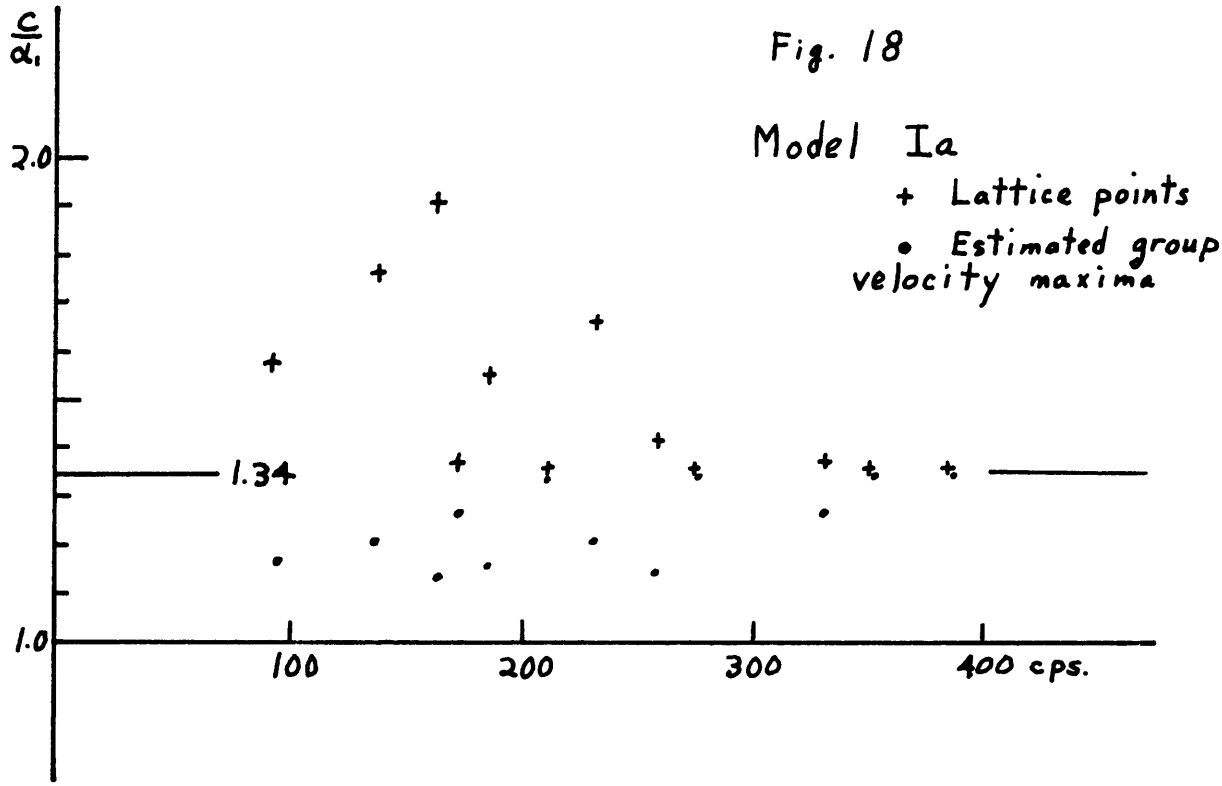
c/α₁
2.0
1.34
1.0
100
200
300
400 cps.
Fig. 18
Model Ia
+ Lattice points
• Estimated group velocity maxima

Chapter III

The four layer model can be considered to represent the type of situation commonly encountered in offshore seismic work. The upper layer represents water; the second and third layers are sediments of increasing consolidation, and the halfspace represents a granitic basement. Two models based on the Buzzards Bay study have been chosen for calculation. Plate-lattice sketches have been prepared, and the phase and group velocity have been obtained by machine calculations for the first model. This chapter consists mainly of discussion of these various curves.

Before time became scarce, it was planned to present twelve different cases, as calculated on the 704, for reference use. These twelve are chosen to be representative of a very broad class of cases, so that they might be of more than academic interest. It is hoped that these curves will be available by late summer of 1959.

The models presented here represent the two extreme situations encountered in Buzzards Bay.

$\alpha_1 = 1.0$	$\rho_1 = 1.0$
$\alpha_2 = 1.04$	$\rho_2 = 1.5$
$\alpha_3 = 1.34$	$\rho_3 = 2.0$
$\alpha_4 = 3.60$	$\rho_4 = 2.65$

Case Ia:
$h_1 = 50$ feet
$h_2 = 20$ feet
$h_3 = 90$ feet

Case Id:
$h_1 = 50$ feet
$h_2 = 90$ feet
$h_3 = 20$ feet

We shall see the effects that thickening and thinning of the sediment layers has on refracted arrivals.

Plate 1 shows the plate-lattice construction for Model la, with composition in the order $(1 + 2) + (3 + 4)$ so that

information about arrivals from the 2 - 3 interface is obtained. On Plate 2, to an appropriate scale, the composition 1 + (2 + (3 + 4) is displayed, yielding predictions on arrivals from the 1-2 interface. Model Id is similarly considered in Plates 3 and 4.

Results obtained from the 704 are tabulated in Appendix III. Modes 1-12 are considered, for ~~both cases~~ case Ia; phase velocity is the independent variable, while frequency and group velocity are given as dependent variables. Frequency is also tabulated in dimensionless form as

$$\gamma = \frac{f H}{\alpha_1}$$

where H is the total thickness of the finite layers.

Plates 5-8 display the group velocity curves for Model Ia as obtained from the tables in Appendix III. Phase velocity curves are omitted for clarity, but these can be easily obtained from the tables. Lattice points from Plates 1-2 are plotted on Plates 5-8 to afford a comparison of the approximate and exact methods.

****

Plates 1-4 illustrate the geometrical factors which limit the existence of proper lattice points. Most generally, the thicknesses of both ensembles generating the plotted set of lattice points control the spacing of group velocity moxima. In Plate 3, the thinness of the 3rd layer causes an extreme spread in its spectral spacing, the first mode curve not approaching 1.34 at all in the range considered. Here it is imperative that high frequencies be received in order for the lower layer to be detected. This condition is

rectified in Plate 1, as the 3rd layer is quite thick. The spectrum of this layer is quite dense, and many lattice points occur at values of c which will generate useful group velocity maxima. The cross-cutting curves, for layers (1 + 2), now control the spacing of lattice points; were both layers to be very thin, the wide spacing of curves for (1+ 2) would create limitations on the existence of useful lattice points. The same general considerations apply in Plates 2 and 4. In the former, due to the thinness of the upper layer, we do not expect refraction arrivals at less than about 800 cps. When this layer is thick, however, the curves q_{23} become quite dense in the useful frequency band, and useful lattice points are generated. In Plate 4 the point $(q_1, q_{23}) = (2,1)$ at 350 cps. would give the lowest frequency wave packet with velocity near 1.04. Note that the control of the water layer is here manifest; if it were thicker, lattice points would occur at substantially lower frequencies, possibly as low as 225 cps.

Another point depicted in Plate 1 is the manner in which the "plateau" in phase velocity at $c = 1.34$ is more extended for the higher modes. This plateau represents the attempt of the phase velocity curve to seek out conditions for mutual reinforcement of waves traveling in the 1.34 layer. With increasing mode number and frequency, naturally, the range of frequencies in which this condition can be nearly met is considerably broadened.

A parameter which is not varied in the figures is the sound velocity in the sediments. One can, however, visualize

the effects very easily. For example, by bringing the velocity of the upper sediment from 1.04 $\rightarrow$ 1.34, the curves for q_{12} are made to cross the 1.34 line more obliquely and the lattice points are spread out more toward higher frequencies. What is more important is that, is the case (not depicted) where the two sediment thicknesses are about the same, the group velocity maxima for the two different refracted events become seriously mixed. Considering the maxima one must interpret when only one layer is significant (for a given useful frequency band) (Plates 5-8), it would be more difficult to make sense out of signals containing group velocity maxima controlled by both layers simultaneously. In terms of wave dispersion the problem is complicated as follows: A group velocity maximum pertaining to the upper of two layers with similar velocities is given by the existence of a node at its upper surface, hence decoupling from the upper layers occurs. Partial decoupling from the underlying layer occurs when an appreciable velocity contrast at the lower surface causes only slight penetration by the signal ($r_j' + 1$ is large). If the velocity contrast at this lower surface is only a few percent, penetration of the underlying layer will be great and it will be a factor in determining the group velocity maxima associated with the layer above it. Problems of this sort are best considered by treating cases of continuous variation of velocity and density, and noting the effects that the various space derivatives of velocity have on the dispersion.

Turning to the group velocity curves, one notices that

m=2 (Plate 6) has a maximum not predicted by the lattices. Furthermore, if the 1.34 layer were very thick, we would have to expect a maximum controlled by this layer even in the first mode. What this means is that in these low modes, particularly the first, conditions may not occur for a pressure node at the upper surface of the layer. If the overlying layer, having a pressure node at its upper surface, is very thin, compared to our thick layer, conditions for a pressure node at the top of the thick layer may be nearly met. As discussed in Chapter 1, this will tend to cause a group velocity maximum, more pronounced as the approximation to a true node becomes better.

In terms of the curves making up the plate-lattice construction, we may think of the curves for layer 3 as being very dense due to its thickness, and the curves for layers (1+2) as being quite sparse. Then the curves for layer 3 in the low modes will come very close to (but not contact) the "0" mode curve for layers (1+2) which is just the vertical coordinate axis. Thus we do not always have a lattice point associated with a low mode maximum, but the virtual contact of the "0" and 1 mode curves can be thought of as a quasi-lattice point associated with a first mode maximum. It is also reasonable to expect maxima to arise under various conditions when near contact between plate curves occurs, even though a lattice point is not produced.

Until the intricacies of this machine calculation are more fully in hand, one must be skeptical of the jagged maxima of small amplitude seen on modes 1, 2, and 3. It is my

feeling that the differentiation built into the program may be inadequate to handle properly some segments of the phase velocity curve, hence the "bump" in the calculated group velocity. These "bumps" will need investigation before they can be accepted as real.

The curves also point up a matter discussed in the next chapter; that many group velocity maxima occur at values of v less than 1.34 (or whatever the layer velocity may be). We also see, however, that the high frequency Airy phase for most modes is very flat and at about $U \approx .90\,\alpha_1$. (Plates 5-8) This could produce a very strong signal immediately after the direct arrival, which, due to its broad spectral composition, would not be in the classical Airy phase form.

While it might be pertinent to make elaborate comparisons of the curves with all of the Buzzards Bay records, it is my feeling that the work would not justify the results. The records do agree with theory to the order of precision obtainable by quick calculation with plate-lattice techniques. At this stage it would be appropriate to carry out more controlled experiments with models to obtain experimental verification of the theory, rather than just non-contradiction.

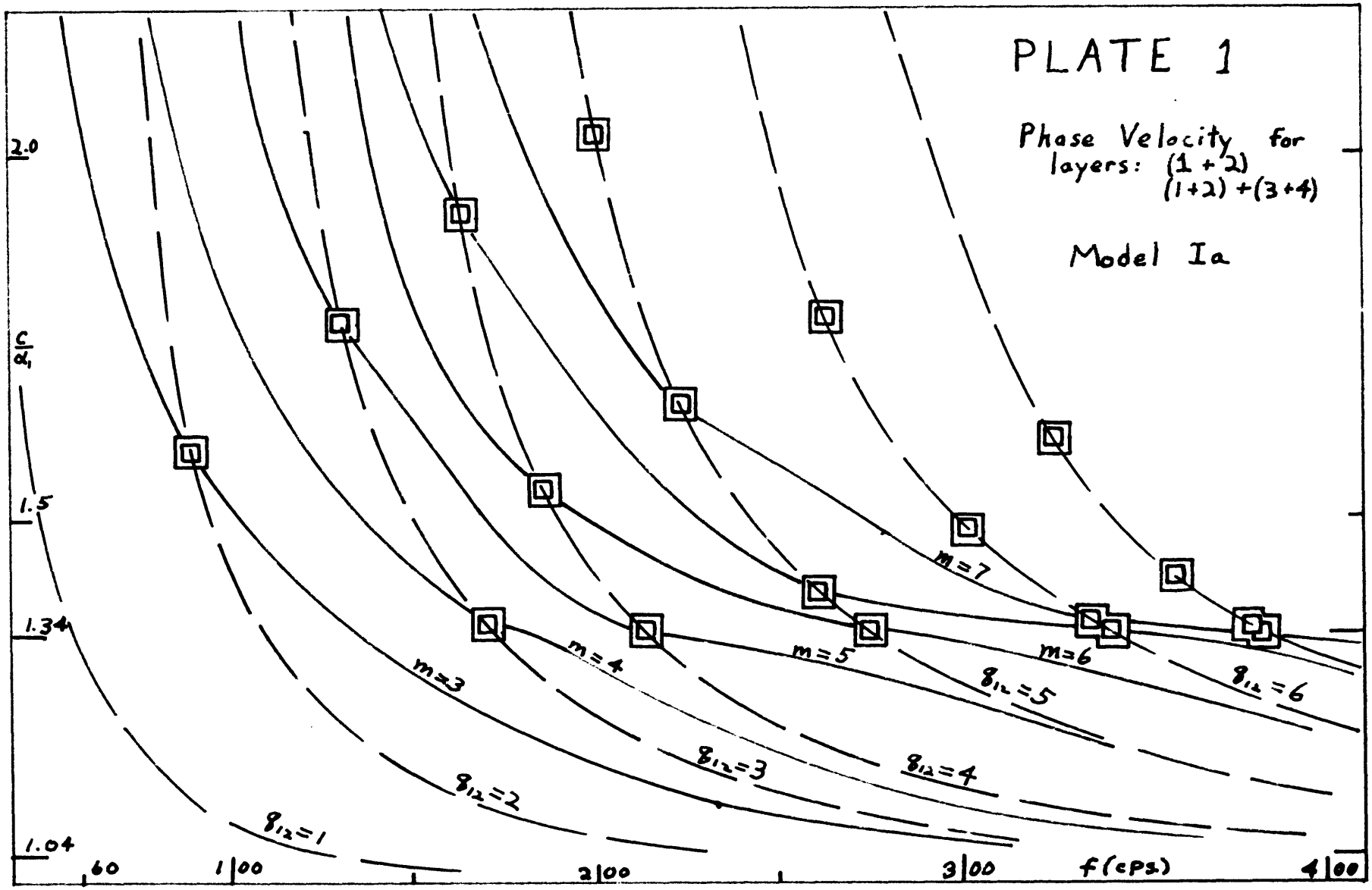
PLATE 1
Phase Velocity for layers: (1 + 2)
(1+2) + (3+4)
Model Ia
2.0
c/α₁
1.5
1.34
1.04
60
1|00
2|00
3|00
f (cps)
4|00
m=3
m=4
m=5
m=6
m=7
g₁₂=1
g₁₂=2
g₁₂=3
g₁₂=4
g₁₂=5
g₁₂=6

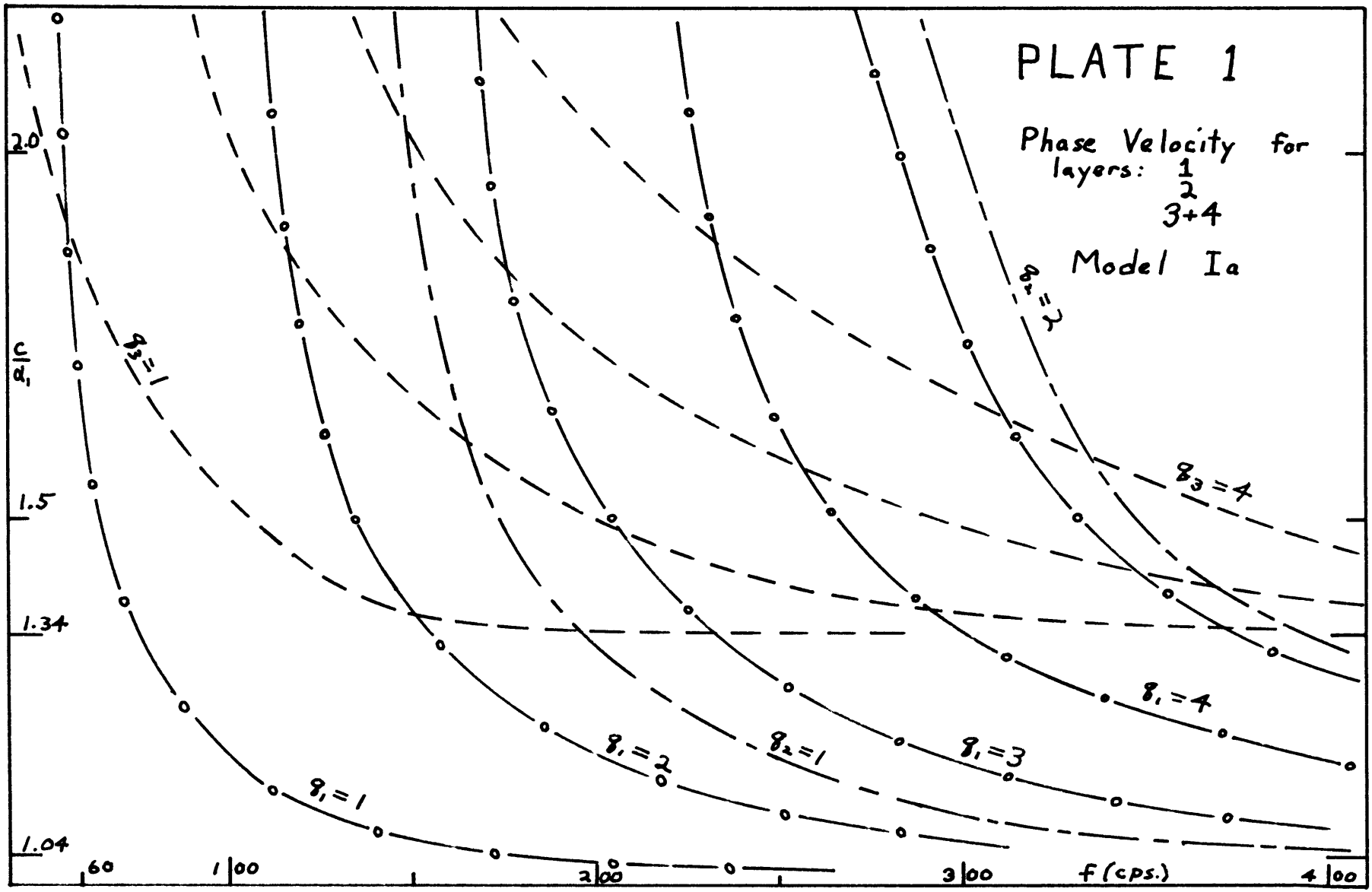
PLATE 1
Phase Velocity for layers: 1
2
3+4
Model Ia
$g_3 = 2$
$g_3 = 4$
$g_3 = 1$
$g_1 = 4$
$g_1 = 3$
$g_2 = 1$
$g_1 = 2$
$g_1 = 1$
$\frac{c}{\alpha_1}$
2.0
1.5
1.34
1.04
60
100
200
300
400
f (cps.)

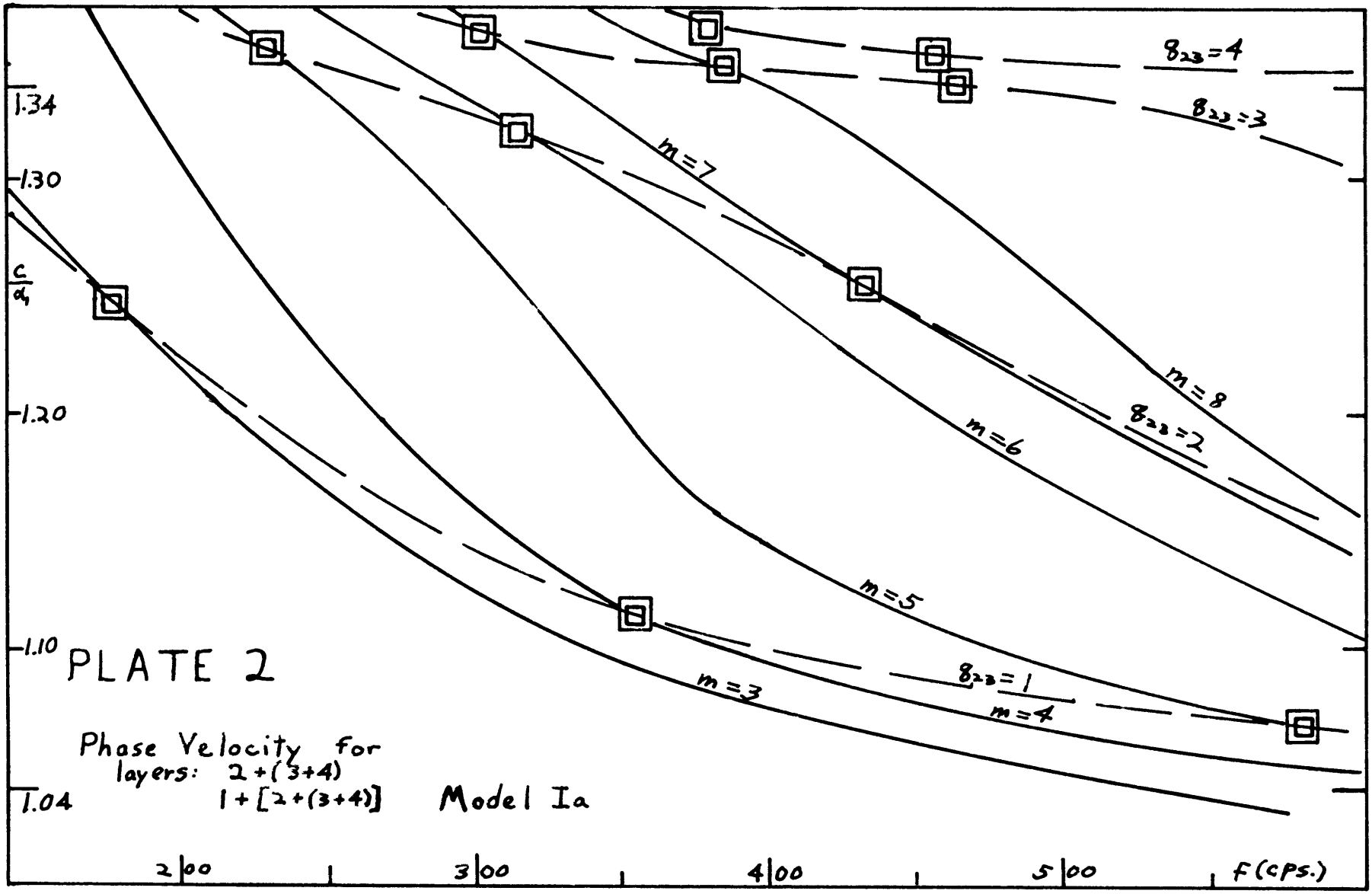

PLATE 2

Phase Velocity for
layers: 2+(3+4)
1+[2+(3+4)]

Model Ia

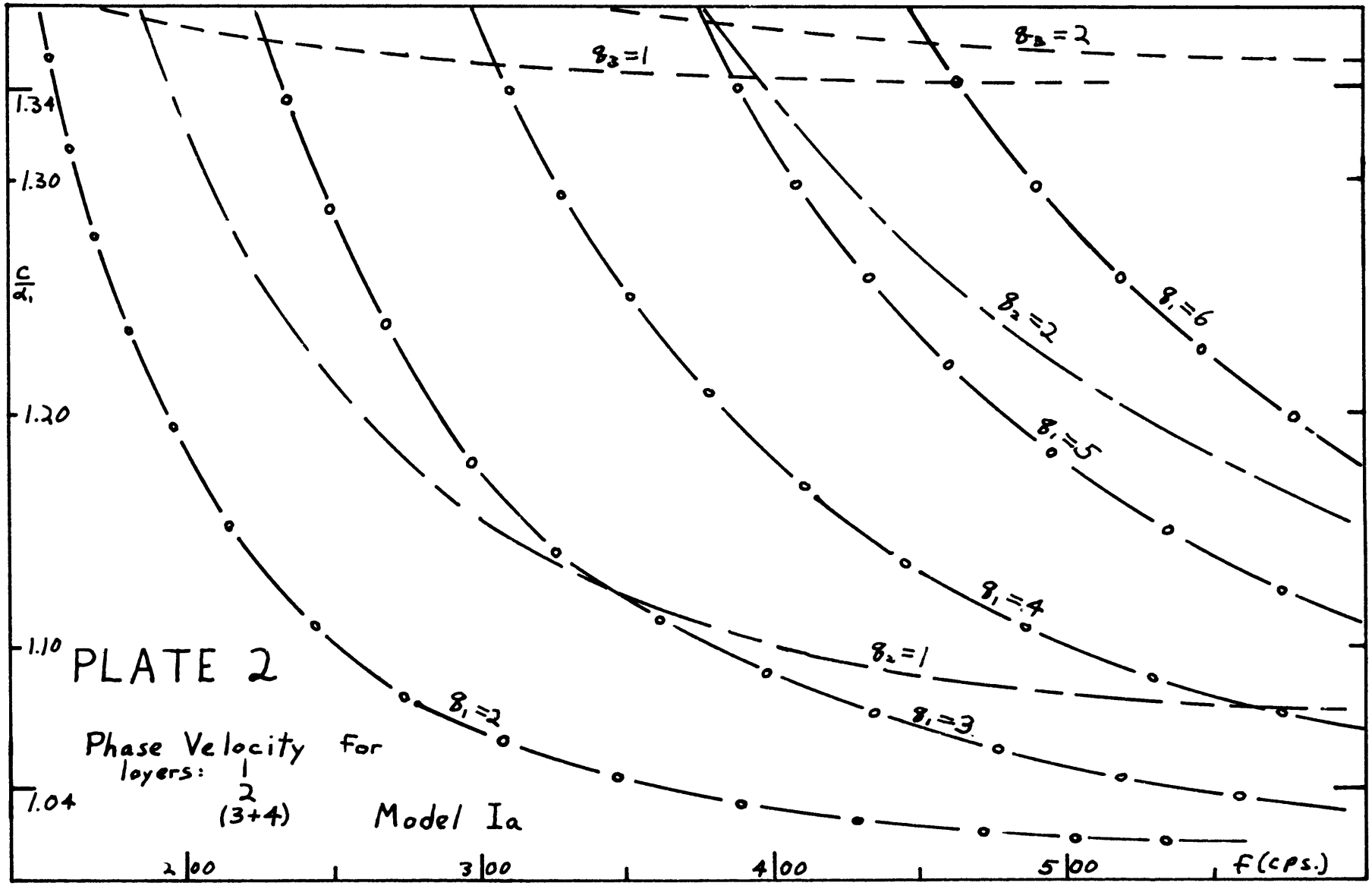
PLATE 2
Phase Velocity for layers: 1, 2, (3+4)
Model Ia
c/α₁
1.34
1.30
1.20
1.10
1.04
2|00
3|00
4|00
5|00
f (cps.)
g₃=1
g₃=2
g₂=2
g₁=6
g₁=5
g₁=4
g₂=1
g₁=3
g₁=2

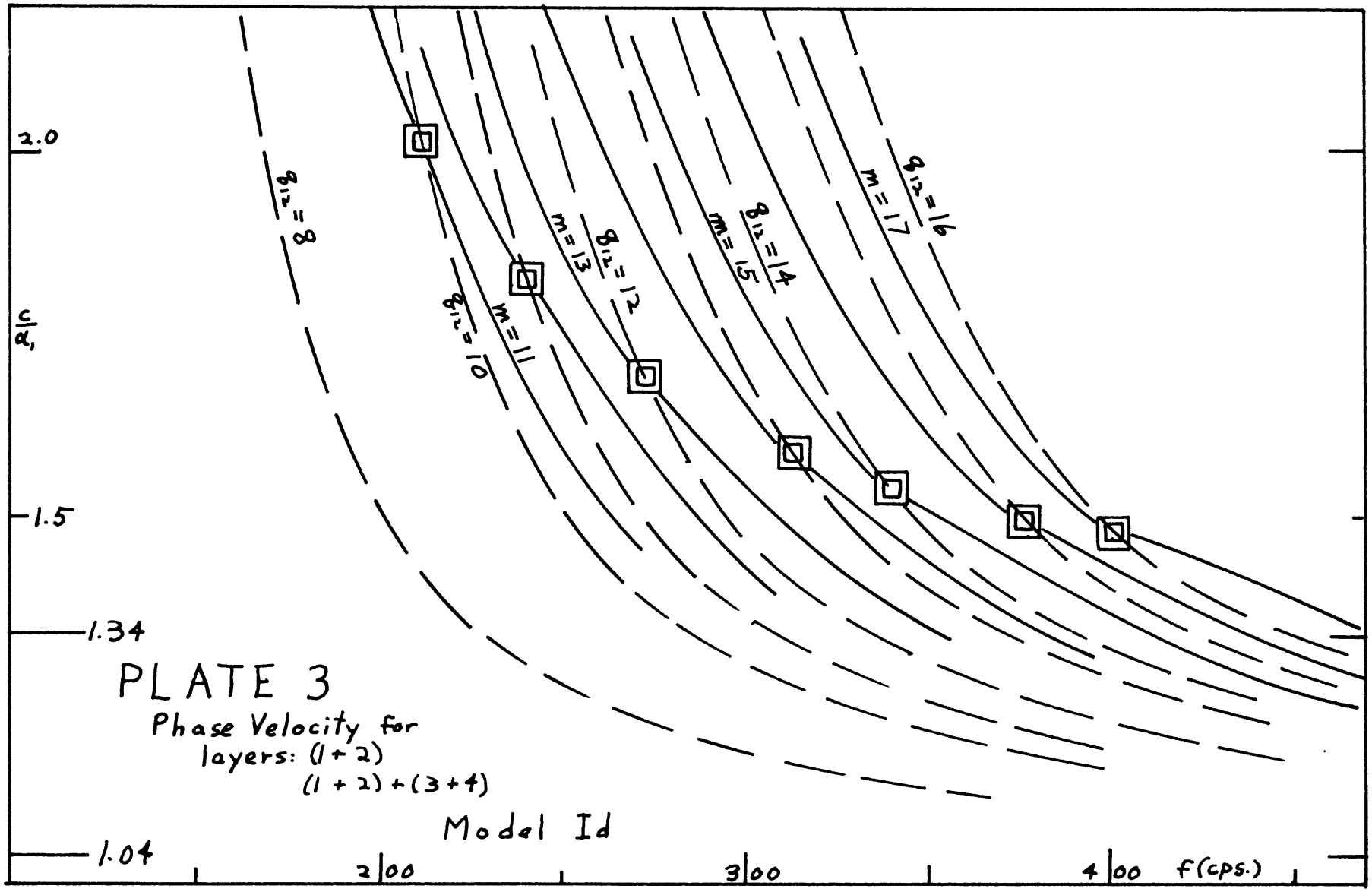

PLATE 3

Phase Velocity for
layers: (1+2)
(1+2)+(3+4)

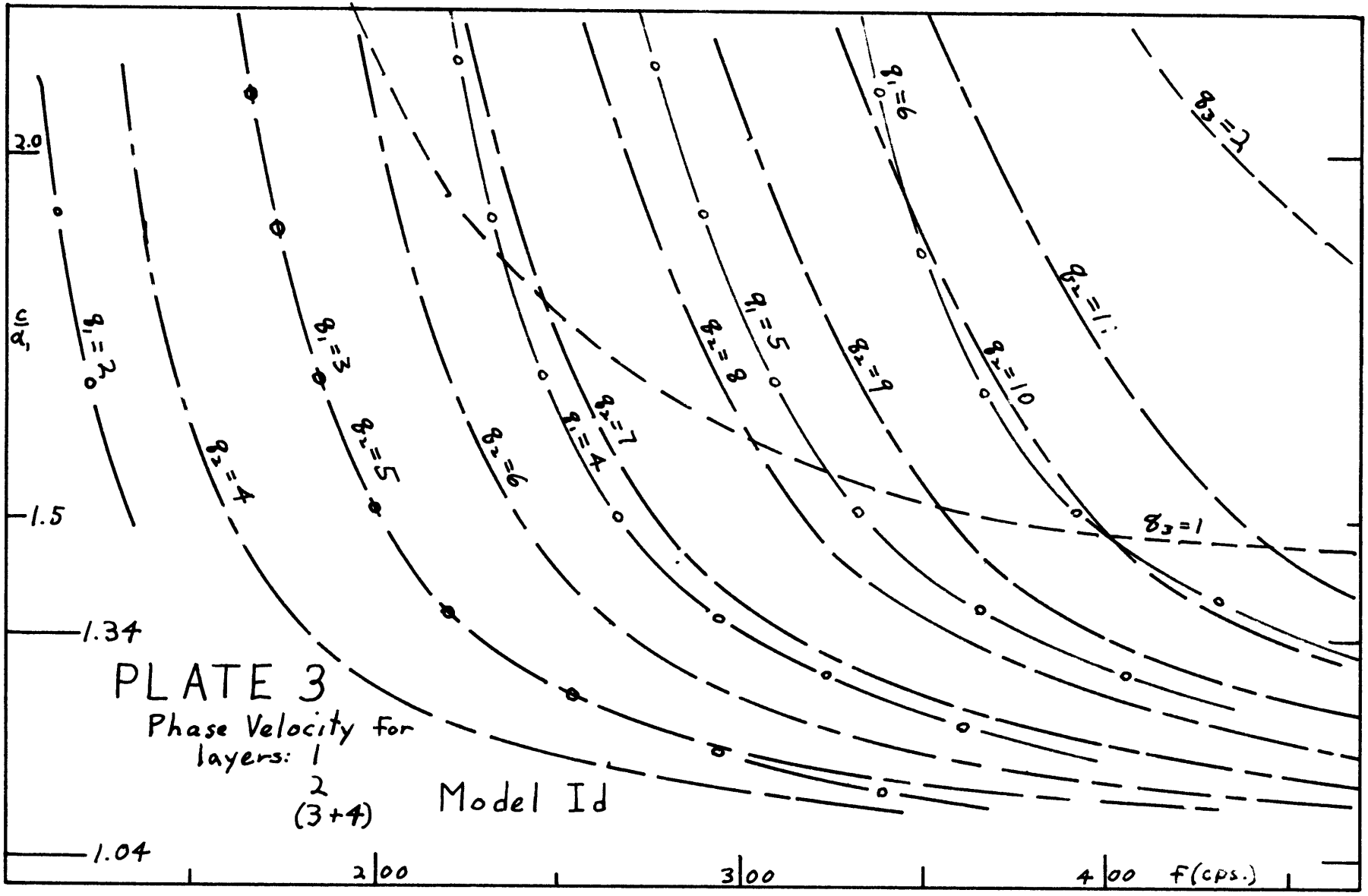

PLATE 3

Phase Velocity for layers: 1
2
(3+4)

Model Id

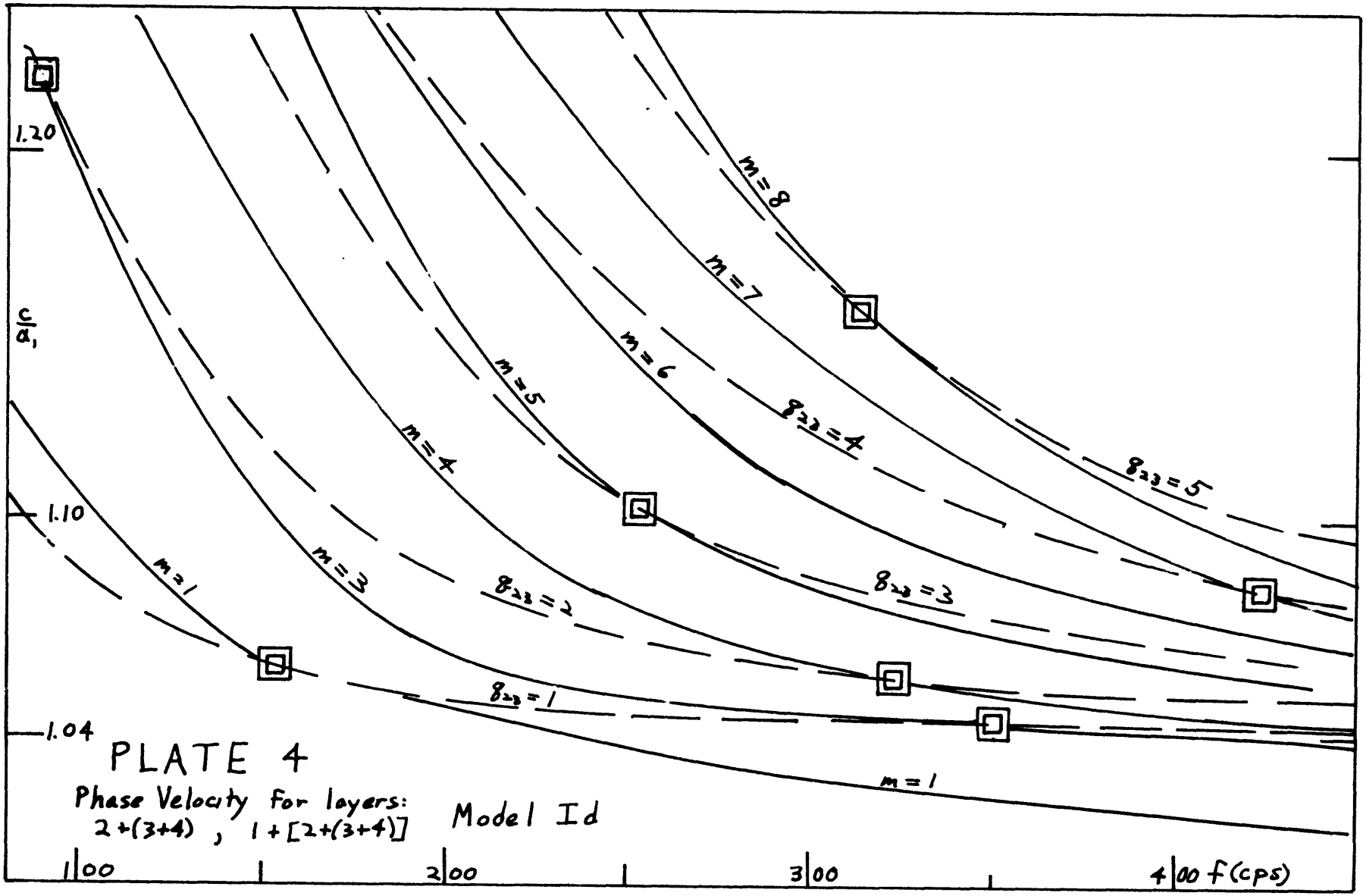

PLATE 4

Phase Velocity for layers:
2+(3+4) , 1+[2+(3+4)]

Model Id

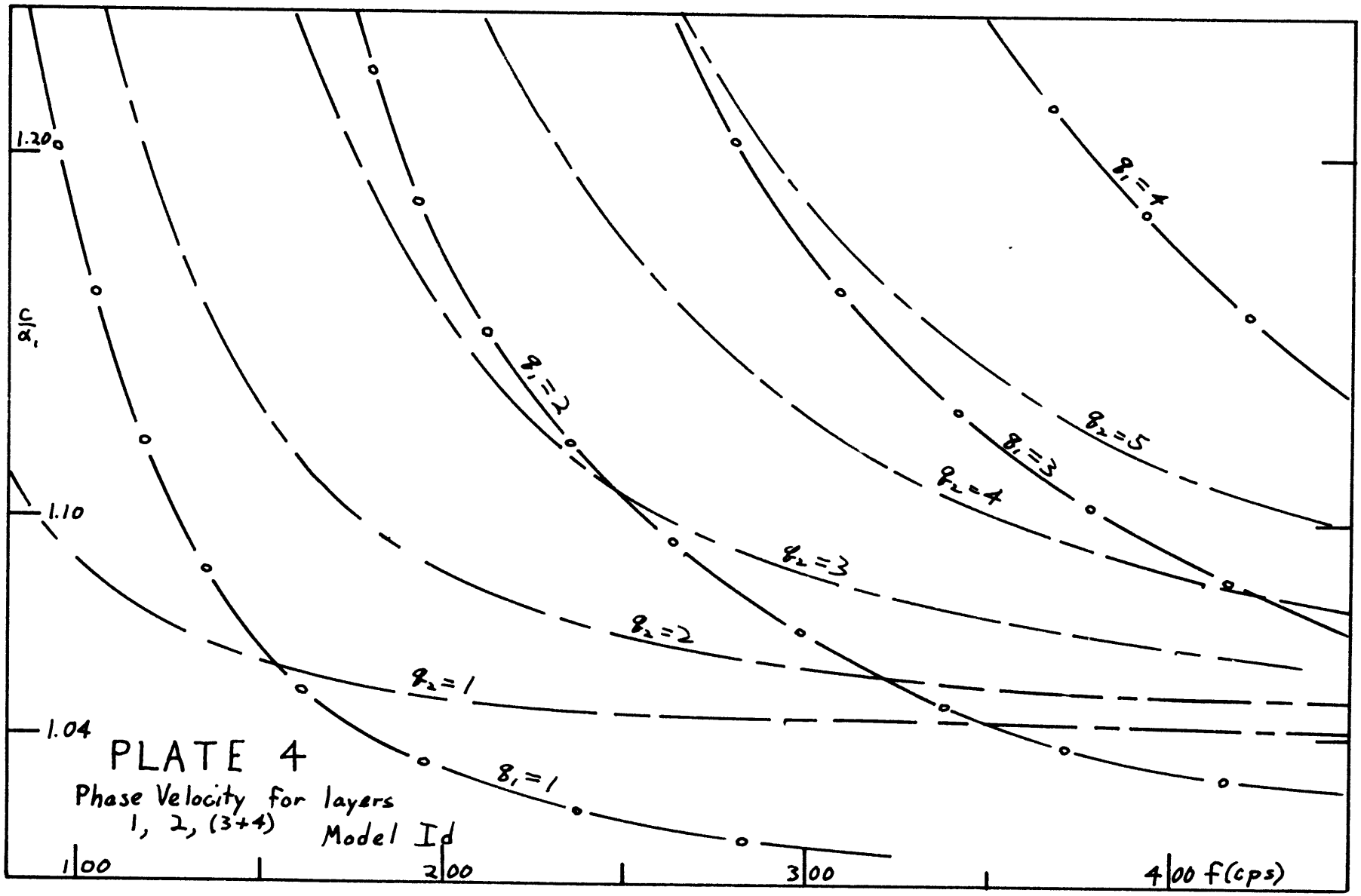

PLATE 4

Phase Velocity for layers 1, 2, (3+4)

Model Id

Chapter IV

Attention must now be brought to bear on the appearance of signals governed by the group velocity considerations of the preceding chapters. We have seen the effect of the thickness of layers or ensembles of layers on existence of the right kind of group velocity maximum for any given mode. We shall now consider the appearance we should expect of second arrivals under typical shooting and receiving conditions.

It commonly happens that the highest modes and frequencies are not evident on a seismic record for several reasons:

1. The receiving transducer is ofter suspended at a depth which selects certain modes in preference to others, a result of the amplitude-depth relation peculiar to each mode. For example, in the Buzzards Bay study, receivers hung about 5 feet below the water surface in 50 feet of water. Basement was about 150 feet deep. The first and second modes were almost entirely absent from the records. Modes in the range 3 to about 8 were strongly emphasized for most frequencies, while higher mode response would be dependent in a periodic manner on the frequency. In this instance ordinary volume attenuation of the high frequencies made observation of high modes very difficult. Anomalous instances occurred in which slacking of the receiver string permitted the transducers to sink to depths

where the first mode overpowered other information.

2. Limited high frequency response of the receiving system will cut out useful high frequency information.

3. Limited resolution (recorder speed) of the galvanometer camera makes high frequency signals hard to pick.

* *

The more interesting and non-trivial results in this chapter will apply in situations where volume attenuation does not remove all the higher modes. The effects described will be most prominent at ranges such that interaction occurs between different refracted signals. We furthermore consider the case where only a few low or medium order modes are effectively present.

The high frequency components which give the impulsive onset of a true Fermat least time signal are absent. Search must be made for wave packets of less distinctive character. Under certain conditions the time scale will be such that the interaction between different wave packets will be slight; in this case picking arrivals is no problem. At the other extreme, in the Buzzards Bay investigation, complicated group velocity functions determined a record shorter than 0.5 seconds. These records were picked by a brute force technique, to be described, which extracted the maximum of information and a hopefully low proportion of

random fluctuations. Figure 16 shows the type of time-distance plot which resulted from this massive picking. Apparent velocities are signified by v.

In Figure 17 the field bounded by the 1.34 and 3.60 lines contains picks associated with the basement refraction arrival and its ray path multiples. The field bounded by the 1.04 and 1.34 lines contains a larger number of picks, with the following features: Those on the 1.04 line are high frequency (around 400 cps.) signals associated with the uppermost sediment layer. The other signals in this field are not easily distinguished by their frequency from the ambient signal of the ground wave. However, the 1.34 line forms a distinct envelope to these points. These are apt to be two linear trends in the points in this field:

1. Lines of apparent velocity $1.04 < v < 1.34$ intercepting near the origin.

2. Cross trends with an echelon appearance, having higher apparent velocities and physically unreasonable high intercepts. We believe that the echelon structure (2) is a result of phase interaction between the signals associated with the 1.34 layer and the frequencies present in the first-arrival ground wave. Evidence from a profile shot in Vineyard Sound where the high velocity sediment appears as a first arrival at several receivers, strongly supports this hypothesis.

The envelope nature of the 1.34 line and the linear

trends (1) of lower velocity are in accord with the group velocity curves displayed in Chapter III for the extreme shallow water case. Certain group velocity maxima will occur at values slightly less than 1.34; others, particularly at lower frequencies, may occur at distinctly lower values. The recording system may very well select more of these spurious lower frequency signals, in favor of the more significant maxima with apparent velocity near 1.34. Thus we have the low velocity signals which correlate from trace to trace, and the fact that none of the arrivals associated with the 1.34 layer appear prior to the appropriate travel time.

We might never be sure whether the signals are spurious, due to low velocity maxima associated with the 1.34 layer, or genuine, resulting from another layer of lower velocity overlying the 1.34 material. If the records are closely spaced, permitting a high density of picks, we are less in danger of missing some layer by masking than we are of predicting a layer that does not exist. The paradox is purely practical; given an optimal receiving system and a lossless medium we could cause genuine arrivals to have an arbitrarily sharp pulse front.

Figure 18 illustrates the preceding discussion; lattice points from case Ia have been transferred from plate I, where they were obtained, and plotted separately. Corresponding values of the group velocity maximum have then been

estimated by graphical differentiation of the appropriate osculating curve in plate I. The lattice points which give rise to the genuine refracted arrival are quite apparent. A considerable number of group velocity maxima, seem to occur in the velocity range 1.12 - 1.18, and it would not be surprising, especially in view of the compressed character of the records, to find strong indications of a refraction arrival with a velocity around 1.15.

Brute force picking, which is necessary to get the most information from a visual inspection of a record, needs some consideration. It is not appropriate, in the case of a highly complicated set of records, to presume that information about sediment layers is irretrievably lost in "noise." Much recent work in seismology has indicated that virtually all features of a seismic record above the instrumental noise level can be explained by careful application of theory to perturbations of the original assumed model. In certain complicated cases, this agreement has been arrived at by hindsight; reflection records in oil prospecting have been found in close agreement with theoretical predictions based on a continuous velocity log.[5] Tatel and Tuve[19] conducted model experiments where complicated Rayleigh wave trains known as "ground roll" were generated by simple surface discontinuities on a solid halfspace. One is led to hope that similar agreement can be found in the present problem by modeling; that is, we want to verify that all the features observed in the field are consequences

of the dispersion of wave trains by relatively simple structures. If this is not the case, it would be appropriate to discover how much perturbation of the simple model was necessary to achieve agreement with actual field seismograms. The present picking technique will depend only on features predicted by the available theory. When a better understanding of all the features found in the field is available, through systematic crosschecks between model and field date, there is reason to hope that picking and calculation of field records can be done with more assurance of reliability.

Given a sequence of seismograms, taken from a receiver spread, with decent resolution of the significant frequencies, one sets out to pick all points that seem to represent changes in the wave train and make a plot in the time-distance plane. The geometrical relationships which these points display are the partial basis for deciding on the "reality" of tentative refraction lines; such geometrical factors will include not only the existence of linear arrays, but some of the other features discussed earlier in this chapter. Since a two-dimensional plot containing a large number of points will always display "line-ups" of points; this matter deserves investigation, namely: given a certain density of points plotted in a region of the plane, how many straight line fits of n or more points should be expected on a statistical basis alone. This additional noise, which is introduced by the act of plotting points, is another

reason why the geometrical relationships mentioned earlier should be kept in mind for supporting evidence.

One brute force technique is to plot all peaks and troughs, filling the plane with + 's and -'s[12]. If not enough traces are available, considerations based on the theory can be brought to bear, and individual points picked with some hope of obtaining useful information. Criteria can be used which tend to select either phase velocities or group velocities, in trace to trace picking of a spread. Picking of identical phase points will define a phase velocity; group velocity is obtained from points of identical frequency. This latter, the more desirable, is also the more difficult to apply, unless it is augmented by some arrival of energy corresponding to a stationary point of group velocity.

To pick an energy arrival, we would require that the trace have a manifestly higher mean square amplitude for one or two cycles after the arrival time. One-half cycle is, of course, insufficient to distinguish the energy arrival from random fluctuations; one cycle is more meaningful, although interpretation of one-cycle wavelets might prove difficult, despite their possibly causal nature. Most of the trace disturbances picked in the Buzzards Bay study were two cycles or more, except where obvious overlap of signals occurred. This energy arrival criterion is useful for identifying a signal; to pick accurately the onset is another matter. If a distinctly different frequency appears, there is no problem.

Otherwise one must rely on picking the change of phase which occurs when a new signal is suddenly superimposed on the ambient variation. This may be completely successful, or of no use at all. Failure can occur when the two signals are entirely in phase, resulting in an indeterminacy of at least half a cycle in the pick. Signals nearly 180° out of phase can produce a null at the true arrival time and a sharp break part of a cycle later. This is the "echelon" effect described earlier in this chapter, the delay imposed on the break being different from trace to trace.

It should not be thought that we would be in danger of picking a phase velocity and wrongly interpreting it, since true second arrivals have their phase and group velocities virtually equal. False arrivals would have associated phase velocities with unreasonable intercepts. It is conceivable that a situation might exist where phase and group velocities might be read with enough precision to reject spurious arrivals, although one should not anticipate finding such a fortuitous occurrence very often.

* *

In a field situation one should apply whatever knowledge or good guesses are available to estimate by the plate-lattice technique the frequencies and modes to be expected in the later arrivals. Hydrophones should be suspended near an antinode of the important modes and (if necessary) sufficiently close to the surface to filter out

the effect of undesired low modes. The information obtainable from a sequence of receivers is much more reliable than that from one receiver; some appropriate scheme is highly desirable. For example, a floating string of receivers, kept under tow by the receiving ship, has been used. This string was, in fact, identical to the array used in shallow water, deep basement reflection prospecting for oil. When more conventional equipment is available, an array can be improvised; depending on the length of the vessel, buoy-slacked hydrophones may be established at intervals from bow to stern, no less than about 40 feet apart, and at the desired depth.

For receiving equipment, a broad-band amplifier, such as the Woods Hole "suitcase" is recommended, feeding into two or three filtered channels for each input. A multichannel galvanometer camera with appropriate paper speed and galvanometer resonance is the best recording device for eventual visual interpretation. The hope is that one or two trial shots would be sufficient to optimize the filter settings. Normally on a multichannel recording, one low frequency trace is used to obtain deepest penetration; one high frequency trace is needed to get an accurate time for the direct arrival. We would be interested in peaking the other channels at the frequencies of the later arrivals.

The existence of a receiving array should make it possible to extract signals from hydrophone noise by correlation techniques. The possibility of establishing such a

method with present FM tape recorders should not be overlooked. Experimental use of a frequency analyzer, such as the "Vibralyzer", when tape recording is available, is strongly suggested. Vibrograms taken in a sound transmission study of Buzzards Bay showed unquestionable evidence of bottom sediment refracted arrivals. These agreed closely with the frequencies observed in the galvanometer camera recordings which constituted the main body of the Buzzards Bay data.

While transmission of energy in the waveguide occurs in the various modes, losses can occur in these "undamped" modes by frequency dependent volume scattering, particularly in the sediment layers. If this mechanism is significant, the signal received at the hydrophone will already be filtered. Since these losses are primarily in the higher frequencies, the signal to noise ratio is adversely affected in these useful frequencies. In a highly lossless situation, there is much to be gained by running at least one high frequency broadband channel, to obtain the effect of as many significant group velocity maxima as possible. If the shot distance is great enough or the sediment thickness sufficient, the high frequency signals will be attenuated and an unfavorable signal to noise ratio ensue. It would then be advisable to record narrow band channels sufficiently below the center of the noise spectrum in an attempt to get wave packets from individual group velocity maxima. The problem in low mode

broad band recording is that severe amplitude contrasts may exist between neighboring modes; our attempt to put all the eggs in one basket by broad band recording is apt to show only the strongly excited modes and render unreadable the wave packets of interest.

Tolstoy[14], in a test of his theory, employed measurements with a constant frequency source and a calibrated hydrophone, taking the mode interaction wavelength as an easily measured quantity. This is a promising new technique; we are here interested, however, in conditions for observation of transients, and mention this only for the sake of completeness.

* *

It is appropriate to ask what effect slight variations in the layer thicknesses might have on the refracted signals. From geological considerations it is often possible to estimate how well or how poorly the earth materials under consideration approximate to a plane waveguide. One would want to know what fundamental limitations the expected perturbations in the geometry would impose on the detection of arrivals. It should be noted that the other types of departure from the ideal model will not be considered. Seldom do inhomogeneities in the layers reach the order of a wavelength in size. The existence of smooth, rather than discontinuous, variation of the physical parameters at a boundary is a problem deserving separate consideration. The geometrical

factors involved in perturbation of a boundary can be interpreted with the use of the plate-lattice analysis, hence we shall devote a few paragraphs to it. A through mathematical analysis will not be attempted, since a really useful and concise formulation of the unperturbed solution is not available yet.

We assume that the sediment layers have variable thickness over the range of a given shot. This amounts to a sequence of perturbations which are imposed in a certain order on the normal modes. For this discussion the perturbations will be considered to be one-dimensional: i.e. linear structures at right angles to the direction of propagation. Any effect these perturbations have on wave character will be a limiting maximum to the effects we would expect from the physically more reasonable case of two-dimensional perturbations. Following usual practice we consider the two limiting types of perturbation: adiabatic and sudden.

In the adiabatic case, with the four layer models in mind, the interface between the second and third layers will be considered to vary gradually over a long range. Such a situation occurs on the continental shelf where relatively homogeneous layers thicken toward the edge of the shelf. Parallel to the structure, less systematic variation of the sediment thicknesses takes place, but in the same gradual manner. Mathematically, this is a limiting

case of the well-known "wedge" problem, which is insoluble by standard eigenfunction techniques. We consider an unperturbed region propagating mth mode plane waves (distant from the source). If the modes of this problem are nearly orthogonal, or if an orthogonal set can be found by change of variable, the perturbed problem would be solved by the mth mode of the perturbed geometry: i.e. in the adiabatic approximation no transitions occur between modes (states). This type of situation would tend to preserve the character of a refracted arrival; naturally the high modes would be the first to suffer, but it is so seldom that we receive the sharp, high frequency edge of the pulse, due to other factors, that this is not a fundamental limitation. As long as the local slope of an interface on the continental shelf is as low as 1:50, the usual situation, modes 1 through 10, which will probably contribute the refracted signals, will propagate with the same weights in the perturbed waveguide. This analysis predicts a set of group velocity maxima in the perturbed geometry with the same number and character as in the unperturbed situation. Hence, the prediction results that the refracted arrivals will propagate with the same apparent velocity as before. The anticipated prediction, that some change in the apparent velocity will occur, due to the slope, is not possible using the present mathematical description. It does not "see" time differences due to variations in the geometry, because the group velocity -- waveguide description is equipped to synthesize pulses only

in the horizontal direction.

Naturally, if the layer thickness is perturbed suddenly, transitions will take place between modes; the transition amplitudes will be proportional to the vector inner product of the mth mode of the unperturbed problem and the nth mode of the perturbed problem. Such a situation was encountered in the Buzzards Bay study; with the aid of a "sparker", graphical reflection records of the sediment were obtained, showing homogeneous bottom sediment overlying glacial drift with a very irregular upper surface. Here we would expect the mth mode signal at the receiver to be due to a series of transitions, appropriately summed. A discontinuously "sudden" perturbation would also induce a reflected wave in the -r direction. This could attenuate refracted signals more than any mode transitions. Under less stringent conditions, more sensible physically, the perturbation might be sudden enough to induce mode transitions yet not have the discontinuity necessary to generate an appreciable reflection.

In cases where the perturbation of an interface has very restricted range, but the least bound on the derivatives is very large, the modes will be slightly less well defined, but the unperturbed modes will still give a good representation of the dispersion. The rough surfaces will permit energy to be radiated into the bottom, effectively increasing

the range attentuation factor. Scattering from rough surfaces is a well-known problem in acoustics, and a straightforward application to this problem should present no difficulties.

Qualitatively we can sum up the effects these mechanisms will have on the significant wave packets composing a refraction arrival. The smearing of the spectral curves by rough boundaries will tend to destroy the critical phase relationships among the different wave packets arriving close to time $t = \frac{r}{\alpha_s}$, and thus tend to blunt the rise of the pulse. This is mentioned only in passing, because the customary attenuation of high frequencies in a real structure more effectively filters the whole transient. If all modes are received, perturbations in any of the boundaries will change only the frequencies of the component wave packets; their transient sum, which is the observed signal, will retain its sharp pulse front. In practice, however, the usual factors will cause the observed signal to be composed from a band of frequencies (usually less than one decade). Any perturbation which will seriously change the number of useful lattice points in this band will threaten the integrity of the pertinent refraction arrival. This is a problem when thin layers are present; the lattice points contributing to the refracted arrival may be only one or two in number. Furthermore the inverse h dependence of the spectrum for single layers makes these lattice points exceedingly sensi-

tive to perturbation of h. Thus a small perturbation may modify the refraction arrival from a thin layer quite profoundly. It is conceivable that in such situations the one or two wave packets would be thoroughly disguised; information would still be present, but would have to be extracted by more sophisticated frequency analysis.

Example Ia has several lattice points in the effective band of, say, 100 to 500 cycles. Here we should expect no trouble in receiving second arrivals if some perturbations were to occur, since sufficiently many lattice points of the perturbed problem would fall in the right band. The effect of many mode transitions, due to a series of perturbations in the shot-receiver interval would be slight in this instance. This is because the part of the observed signal due to modes is due only to the modes of that part of the waveguide local to the receiver, and we have indicated the acceptability of lattice points in these modes. If a series of transitions has occurred, two other effects are apt to reduce the amplitude of the wave packets:

1. The probability of back reflection, previously mentioned, if the perturbations are sharp enough.

2. Broadening of the range of modes originally the explosive source favored a certain wide range of modes; i.e. the source spectrum always determines the relative excitation of different frequencies. A series of mode transitions may excite modes outside of the

originally significant range, hence the relative excitation of the few observed modes must decrease. This cannot mean that new frequencies are introduced; it is the wave numbers and phase velocities that change, subject to the period equation.

It is now apparent, in general, that we must expect more difficulties in observing refraction arrivals when geometries with perturbed layers are considered. In a great many cases, however, much or most of the useful information is retained in the signal. The need for mathematical investigation is apparent, and many possibilities for this have been suggested.

Conclusions

The plate-lattice analysis enables one to obtain useful information about the transient signal and, particularly, the refraction arrivals from layers above the basement. Information of a sepctral nature, such as the central frequencies of the wave-packets, is easily come by. The phenomena of interaction between a second and first arrival and the existence of group velocity maxima with spurious velocities are of the same type. As remarked before analysis into modes makes possible synthesis of a transient signal traveling in the r direction only. However, in order to rigorously account for second-arrival transients, the theory must incorporate travel times in the overlying layers. The approximations inherent in the present work imply a zero intercept for the refraction lines. Thus, we have learned a good deal about the refracted arrivals insofar as frequency is concerned, particularly since the recording system and transmitting medium act as a bandpass filter; we have not yet accounted for intercepts and changes in apparent velocity due to slight perturbations in layer thickness. A complete theory would be desirable which handled refraction arrivals from upper layers at short ranges, indeed, in cases where they occur as first arrivals.

Press[16] has suggested that an expansion of the integrand of the formal integral solution could be performed which would give a fairly concise expression for the phenomenon

of interest. I have not given the matter much consideration beyond this, but I feel it very unlikely that any attempt to mathematically sum all the contributions from group velocity maxima would meet with success, especially in view of the limitations expressed above. Beside involving complicated double sums of functions like the reverse Airy phase, this would always leave considerable doubt about the physical meaning of the answer. For the time being we must be content with knowing that the main body of a refracted pulse comes from the group velocity maxima and that useful knowledge about the frequencies present is readily available from the same theory.

Appendix I

Table of Symbols

α_i	compressional wave velocity in the ith layer
h_i	thickness of the ith layer
ρ_i	density of the ith layer
z	vertical coordinate
r	horizontal coordinate
c	horizontal phase velocity
ω	angular frequency
f	frequency $= \frac{\omega}{2\pi}$
k	horizontal wave number $= \frac{\omega}{c}$
r_i	vertical wave number in ith layer $= \sqrt{\frac{\omega^2}{\alpha_i^2} - \frac{\omega^2}{c^2}}$
r_i'	imaginary vertical wave number $= \sqrt{\frac{\omega^2}{c^2} - \frac{\omega^2}{\alpha_i^2}}$
U	group velocity $= \frac{d\omega}{dk}$
v	any apparent velocity
t	time
m	mode index for entire waveguide
$q_{ij\cdots l}$	mode index for waveguide consisting of layers: i, j, ...l
$\mathcal{R}_{j,j+1}^{(n-j)}$	generalized Rayleigh reflection coefficient for layers (j + 1, j + 2, ...,n), j being the medium of incidence.
$R_{j,j+1}$	Rayleigh reflection coefficient at the j, j + 1 interface, j being the medium of incidence. $= \frac{r_j \rho_{j+1} - r_{j+1} \rho_j}{r_j \rho_{j+1} + r_{j+1} \rho_j}$
$\chi_{j,j+1}^{(n-j)}$	half angle of phase change induced by reflection at the j, j + 1 interface in the waveguide. $\mathcal{R}_{j,j+1}^{(n-j)} = e^{2i\chi_{j,j+1}^{(n-j)}}$

Appendix II

An Outline of the Buzzards Bay Seismic Refraction Study

Bunce, E. T., Phinney, R. A., and Pooley, R. N.: Seismic Refraction Observations in Buzzards Bay, Mass. Presented at the 40th annual meeting of the American Geophysical Union, Washington, D. C., May 5, 1959. Paper in preparation.

Abstract

Detailed seismic refraction measurements have been made in this shallow-water area. A towed buoyant cable carrying 12 detectors at 100 ft. intervals was used. First arrivals from the basement are found on all records. Observed velocities range from 5.1 to 5.7 km./sec., and calculated depths range from 18 to 75 m. below sea level. In a well-defined area of at least seven square miles, substantially lower basement velocities of 4.2 to 4.5 km./sec. are found. Both observed basement velocities are suggestive of the granite gneiss complex observed in outcrops on the western side of Buzzards Bay. Indicated sedimentary velocities, which range from 1.52 to 2.4 km./sec., are associated with second or later arrivals. Complicated patterns of dispersive waves restrict the accuracy with which these later arrivals can be interpreted. This uncertainty, plus the known glacial character of the sediments, is more than sufficient to account for the poor correlation of sedimentary velocities.

* *

Comments

This study, which was started in the summer of my Junior year, has been for me a complete course in record reading, instrumentation, and theory. It appears that the records obtained were unique in refraction work, for the short time and distance scales involved. The departure of the sediment-sediment interface from a plane also must have set some kind of a record for our presumptuousness in trying to "shoot" it by refraction.

The presently available results from the Buzzards Bay study involve delineation of the basement topography, and it was with some confidence that we were able to present profiles of the basement surface. Although our knowledge of the sediments was less than unique, we felt that we had achieved some intimacy with them after reading over 200 high quality records for sediment arrivals. Several features appeared in the plots which repeated from profile to profile and seemed to warrant looking into. This behavior of the plotted points is explained in Chapter IV of this thesis. One can imagine, for example, our initial surprise when the first good record obtained showed good correlation of a wave packet on four adjacent traces, with velocity around 10,000 ft./sec. and a time intercept four times greater than the intercept from the crystalline basement.

A couple of fortuitous bits of data not included in

the original program proved to be of real value in pinning down these sediments. After a couple of tries, a usable sparker record was obtained which showed without question the structure of the sediments: A fine grained homogeneous clay or silt which formed the flat bottom of the Bay overlay, across a very irregular interface, material which scattered the sound so distinctively that its glacial character was considered proven. The basement, only a few fathoms beneath the drift, was not seen at all on the sparker records due to this excessive scattering. Because of the shallow depth to basement and noting the important role glaciation played in the area, we feel that the drift directly overlies the basement. We were also fortunate in receiving from Dr. Charles B. Officer, Jr., records which were shot in Vineyard Sound, only about 3 miles southwest of some of the Buzzards Bay work. When these were plotted, the structure of the sediment was made obvious, due to first-arrival date, and the envelope nature of the second arrival part of the high velocity sediment line was explicited.

Another feature we found, which was to be explained by the Tolstoy theory, was the occurence of a physically unbelievable number of good sediment refraction lines. It now appears that only the greatest and the least of these were real, corresponding to the two sediments just mentioned, while all the others were due to group velocity maxima governed by the higher velocity layer. One record showed this feature remarkably well; no less than six sediment

layers seemed to lie in a 100 foot vertical interval.

Needless to say, the method of picking signals, which is discussed in Chapter IV, was not laid out after shrewd consideration of the present theory. It was, however, soundly based on the fundamentals of the way energy travels in a wave, and has to make some kind of sense in terms of any reasonable theory. We were gratified that the time-distance plots did not look like scatter diagrams, but that certain features stood out on a large number of shots. The present thesis was undertaken in an effort to understand these features and learn more about the nature of mode propagation.

	m = 1			m = 2			m = 3		
c	f		U	f		U	f		U
3.6000	12.69	0.4077	0.	27.08	0.8702	0.	49.69	1.5965	0.
3.5000	13.23	0.4250	1.562	27.57	0.8859	0.985	50.35	1.6177	0.824
2.5000	15.97	0.5131	0.932	31.04	0.9972	0.771	55.66	1.7883	0.684
1.8000	20.76	0.6669	0.936	39.51	1.2694	0.995	66.91	2.1497	0.816
1.6500	23.04	0.7404	0.941	45.13	1.4500	1.079	72.70	2.3358	0.881
1.5000	26.57	0.8538	0.941	57.63	1.8516	1.162	83.35	2.6779	0.998
1.4500	28.20	0.9060	0.943	65.59	2.1073	1.167	90.82	2.9179	1.113
1.4000	30.18	0.9697	0.936	75.86	2.4373	1.113	108.20	3.4762	1.225
1.3900	30.62	0.9838	0.934	77.94	2.5040	1.091	113.99	3.6625	1.224
1.3800	31.08	0.9985	0.933	79.95	2.5686	1.067	119.95	3.8537	1.197
1.3700	31.56	1.0138	0.932	81.88	2.6308	1.043	125.01	4.0163	1.137
1.3650	31.80	1.0218	0.931	82.82	2.6610	1.032	127.07	4.0826	1.101
1.3600	32.06	1.0299	0.930	83.75	2.6907	1.017	128.87	4.1405	1.065
1.3550	32.31	1.0381	0.929	84.68	2.7205	1.006	130.48	4.1921	1.029
1.3500	32.57	1.0465	0.929	85.57	2.7494	0.998	131.96	4.2398	1.005
1.3460	32.79	1.0535	0.951	86.28	2.7722	0.982	133.06	4.2751	0.986
1.3420	33.01	1.0605	0.925	86.99	2.7949	0.981	134.11	4.3089	0.966
1.3200	38.53	1.2379	1.026	93.52	3.0045	1.047	141.97	4.5612	1.023
1.2800	43.03	1.3825	1.006	104.92	3.3709	0.999	158.54	5.0936	1.003
1.2400	48.41	1.5554	0.978	116.55	3.7444	0.939	177.13	5.6908	0.955
1.2000	54.73	1.7582	0.948	128.85	4.1397	0.905	197.31	6.3391	0.920
1.1600	62.34	2.0028	0.927	143.81	4.6204	0.901	221.80	7.1261	0.913
1.1200	72.52	2.3299	0.925	165.05	5.3028	0.916	256.76	8.2494	0.926
1.1000	79.51	2.5546	0.931	180.33	5.7937	0.928	282.18	9.0660	0.937
1.0800	88.92	2.8569	0.941	201.47	6.4731	0.941	317.67	10.2062	0.949
1.0700	95.10	3.0553	0.947	215.63	6.9277	0.949	341.50	10.9719	0.955
1.0600	102.84	3.3040	0.954	233.54	7.5033	0.956	371.61	11.9393	0.961
1.0500	112.91	3.6277	0.961	257.17	8.2626	0.964	410.98	13.2040	0.966
1.0440	120.66	3.8766	0.965	275.46	8.8502	0.968	441.09	14.1715	0.970
1.0200	185.05	5.9455	0.985	426.44	13.7008	0.985	678.11	21.7866	0.984

MODEL Ia

	m = 4			m = 5			m = 6		
c	f		U	f		U	f		U
3.6000	67.33	2.1633	0.	87.01	2.7954	0.	105.03	3.3745	0.
3.5000	68.03	2.1858	0.712	87.71	2.8179	0.595	106.02	3.4062	0.684
2.5000	74.62	2.3975	0.678	94.56	3.0381	0.583	116.50	3.7430	0.698
1.8000	91.29	2.9329	0.896	111.13	3.5705	0.811	142.90	4.5912	0.895
1.6500	100.93	3.2428	0.938	121.76	3.9118	0.951	155.26	4.9881	0.817
1.5000	116.15	3.7316	0.919	148.82	4.7813	1.136	172.46	5.5410	0.886
1.4500	123.05	3.9535	0.941	166.51	5.3498	1.094	185.66	5.9650	1.127
1.4000	134.16	4.3103	1.116	180.39	5.7957	0.906	226.44	7.2752	1.204
1.3900	138.98	4.4653	1.195	182.81	5.8733	0.901	234.71	7.5408	1.109
1.3800	147.35	4.7341	1.258	185.47	5.9588	0.947	240.02	7.7115	0.994
1.3700	162.30	5.2146	1.289	189.36	6.0837	1.096	244.11	7.8428	0.943
1.3650	172.43	5.5401	1.286	193.60	6.2202	1.224	246.15	7.9085	0.957
1.3600	181.02	5.8159	1.235	204.63	6.5746	1.299	248.58	7.9866	1.031
1.3550	185.39	5.9564	1.111	226.80	7.2869	1.313	253.51	8.1449	1.221
1.3500	187.78	6.0331	0.999	244.70	7.8618	1.217	279.47	8.9789	1.316
1.3460	189.22	6.0794	0.976	248.43	7.9817	1.043	297.83	9.5688	1.204
1.3420	190.45	6.1190	0.908	250.48	8.0477	0.961	302.04	9.7042	1.041
1.3200	197.73	6.3526	0.917	259.73	8.3446	0.894	315.42	10.1340	0.936
1.2800	212.95	6.8418	0.919	277.21	8.9063	0.875	339.56	10.9094	0.900
1.2400	231.80	7.4475	0.912	297.56	9.5601	0.867	365.98	11.7585	0.874
1.2000	255.14	8.1972	0.907	322.71	10.3681	0.872	397.14	12.7597	0.870
1.1600	286.02	9.1894	0.914	356.58	11.4562	0.889	438.20	14.0788	0.885
1.1200	332.82	10.6929	0.936	408.03	13.1094	0.918	499.26	16.0403	0.910
1.1000	368.72	11.8464	0.951	447.29	14.3708	0.937	544.17	17.4835	0.925
1.0800	421.86	13.5538	0.965	507.02	16.2897	0.963	608.00	19.5341	0.944
1.0700	459.17	14.7525	0.971	553.32	17.7774	0.978	653.24	20.9878	0.958
1.0600	506.61	16.2765	0.972	622.77	20.0087	0.991	720.12	23.1364	0.983
1.0500	566.28	18.1936	0.971	718.37	23.0802	0.983	855.43	27.4836	1.004
1.0440	609.69	19.5885	0.972	779.11	25.0315	0.974	948.26	30.4661	0.979
1.0200	930.74	29.9032	0.983	1183.45	38.0226	0.982	1436.17	46.1421	0.982

MODEL Ia

	m = 7			m = 8			m = 9		
c	f		U	f		U	f		U
3.6000	127.51	4.0966	0.	142.71	4.5850	0.	166.96	5.3641	0.
3.5000	128.22	4.1195	0.482	143.83	4.6211	0.621	167.92	5.3950	0.501
2.5000	136.96	4.4002	0.546	157.43	5.0579	0.689	179.91	5.7801	0.545
1.8000	158.99	5.1082	0.825	192.03	6.1696	0.829	210.11	6.7504	0.841
1.6500	176.04	5.6560	1.011	207.57	6.6691	0.802	232.24	7.4614	0.984
1.5000	215.00	6.9077	1.028	235.59	7.5690	1.062	269.03	8.6437	0.927
1.4500	229.02	7.3581	0.905	262.39	8.4302	1.129	288.55	9.2706	1.090
1.4000	248.34	7.9788	1.166	288.83	9.2797	0.998	331.07	10.6367	0.996
1.3900	260.84	8.3803	1.243	294.80	9.4714	1.076	336.42	10.8088	0.944
1.3800	278.10	8.9349	1.230	306.11	9.8349	1.222	341.96	10.9866	0.995
1.3700	290.30	9.3271	1.100	330.61	10.6220	1.250	354.28	11.3825	1.241
1.3650	294.06	9.4478	1.039	339.57	10.9099	1.138	374.27	12.0248	1.296
1.3600	297.34	9.5530	1.016	344.10	11.0554	1.012	397.78	12.7800	1.237
1.3550	300.91	9.6677	1.071	347.43	11.1625	0.970	404.50	12.9959	0.987
1.3500	309.99	9.9594	1.276	351.33	11.2876	1.088	407.90	13.1053	0.925
1.3460	344.93	11.0821	1.288	379.10	12.1800	1.327	412.34	13.2480	1.193
1.3420	351.32	11.2875	1.016	410.27	13.1815	1.006	468.76	15.0605	1.147
1.3200	364.55	11.7124	0.904	423.00	13.5903	0.846	484.61	15.5699	0.855
1.2800	391.49	12.5780	0.909	448.42	14.4071	0.856	513.40	16.4949	0.844
1.2400	424.32	13.6329	0.897	480.39	15.4341	0.867	547.63	17.5945	0.846
1.2000	464.02	14.9083	0.890	521.95	16.7694	0.881	591.04	18.9893	0.860
1.1600	515.90	16.5751	0.898	579.92	18.6320	0.903	650.88	20.9117	0.885
1.1200	592.14	19.0247	0.917	670.93	21.5561	0.931	744.01	23.9038	0.919
1.1000	647.38	20.7993	0.928	740.53	23.7920	0.944	817.55	26.2667	0.943
1.0800	723.57	23.2472	0.941	837.58	26.9103	0.951	933.36	29.9874	0.967
1.0700	774.61	24.8871	0.950	900.39	28.9281	0.953	1016.86	32.6703	0.970
1.0600	841.28	27.0290	0.963	977.60	31.4089	0.958	1115.25	35.8313	0.964
1.0500	962.98	30.9390	1.007	1086.45	34.9059	0.983	1234.42	39.6600	0.969
1.0440	1115.71	35.8462	0.989	1277.39	41.0405	1.008	1417.56	45.5440	1.024
1.0200	1688.89	54.2616	0.982	1941.61	62.3811	0.981	2194.33	70.5006	0.981

MODEL Ia

	m = 10			m = 11			m = 12		
c	f		U	f		U	f		U
3.6000	182.53	5.8644	0.	203.16	6.5273	0.	222.67	7.1542	0.
3.5000	183.68	5.9013	0.539	204.26	6.5625	0.491	224.07	7.1990	0.542
2.5000	199.08	6.3962	0.637	219.29	7.0454	0.578	242.51	7.7914	0.609
1.8000	237.01	7.6147	0.784	261.94	8.4157	0.878	282.05	9.0618	0.745
1.6500	256.49	8.2407	0.874	286.90	9.2176	0.848	307.70	9.8861	0.987
1.5000	303.62	9.7550	1.021	324.58	10.4282	1.061	364.40	11.7077	0.855
1.4500	322.56	10.3633	0.903	364.79	11.7203	1.144	384.16	12.3425	1.048
1.4000	367.22	11.7981	1.245	394.13	12.6628	0.997	444.63	14.2853	0.972
1.3900	386.59	12.4205	1.165	407.26	13.0846	1.229	451.61	14.5095	0.962
1.3800	395.49	12.7065	0.946	437.75	14.0643	1.254	462.73	14.8670	1.175
1.3700	401.32	12.8938	0.929	455.67	14.6401	1.015	495.76	15.9279	1.215
1.3650	405.26	13.0205	1.068	459.90	14.7759	0.966	504.98	16.2244	1.066
1.3600	420.72	13.5170	1.295	464.62	14.9275	1.057	510.68	16.4075	1.014
1.3550	456.48	14.6660	1.261	483.59	15.5371	1.300	518.79	16.6678	1.192
1.3500	465.34	14.9507	1.001	512.34	16.4606	1.129	562.07	18.0583	1.247
1.3460	469.26	15.0765	1.040	517.72	16.6336	1.032	568.63	18.2692	0.954
1.3420	517.26	16.6187	1.255	569.19	18.2873	1.313	627.26	20.1530	1.332
1.3200	537.55	17.2708	0.892	588.10	18.8949	0.852	648.49	20.8351	0.821
1.2800	573.64	18.4304	0.874	624.81	20.0743	0.870	684.30	21.9855	0.833
1.2400	615.07	19.7612	0.860	671.41	21.5713	0.876	729.41	23.4348	0.849
1.2000	665.33	21.3761	0.863	730.55	23.4714	0.881	788.98	25.3488	0.871
1.1600	732.59	23.5372	0.882	809.99	26.0238	0.894	873.83	28.0749	0.899
1.1200	833.50	26.7791	0.909	927.16	29.7883	0.913	1008.83	32.4123	0.928
1.1000	908.63	29.1928	0.927	1011.57	32.5003	0.925	1109.96	35.6613	0.937
1.0800	1020.46	32.7858	0.955	1128.88	36.2694	0.942	1245.49	40.0157	0.943
1.0700	1109.84	35.6576	0.977	1211.49	38.9234	0.958	1333.61	42.8469	0.949
1.0600	1242.83	39.9303	0.981	1344.08	43.1833	0.991	1451.97	46.6497	0.971
1.0500	1389.02	44.6271	0.967	1544.04	49.6077	0.972	1694.16	54.4309	0.987
1.0440	1530.10	49.1599	1.017	1669.98	53.6541	0.993	1831.57	58.8455	0.978
1.0200	2447.05	78.6201	0.981	2699.77	86.7396	0.981	2952.49	94.8591	0.981

MODEL Ia

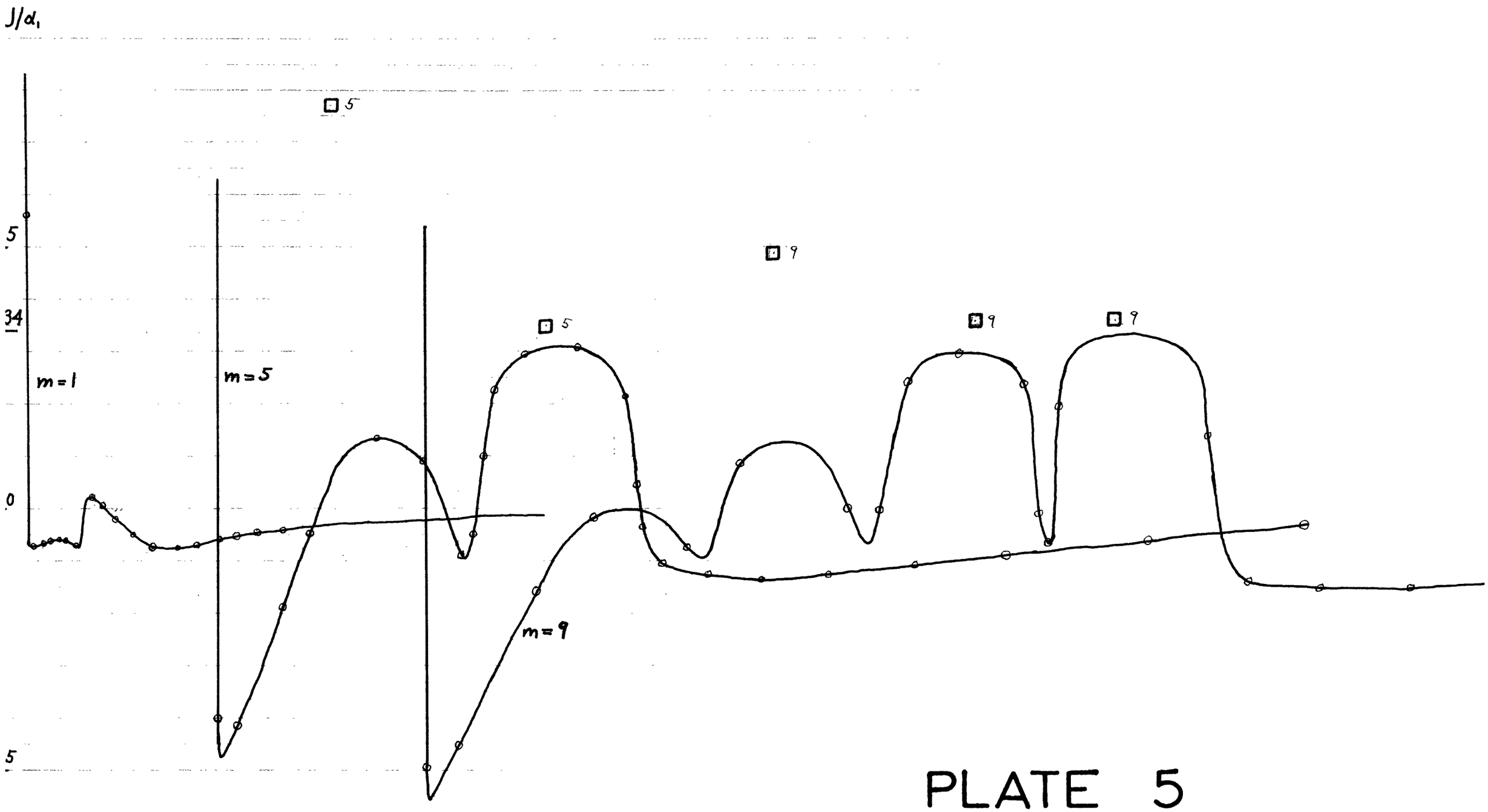

PLATE 5

Model Ia : Group Velocity

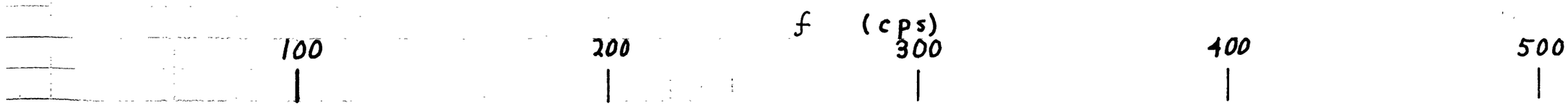

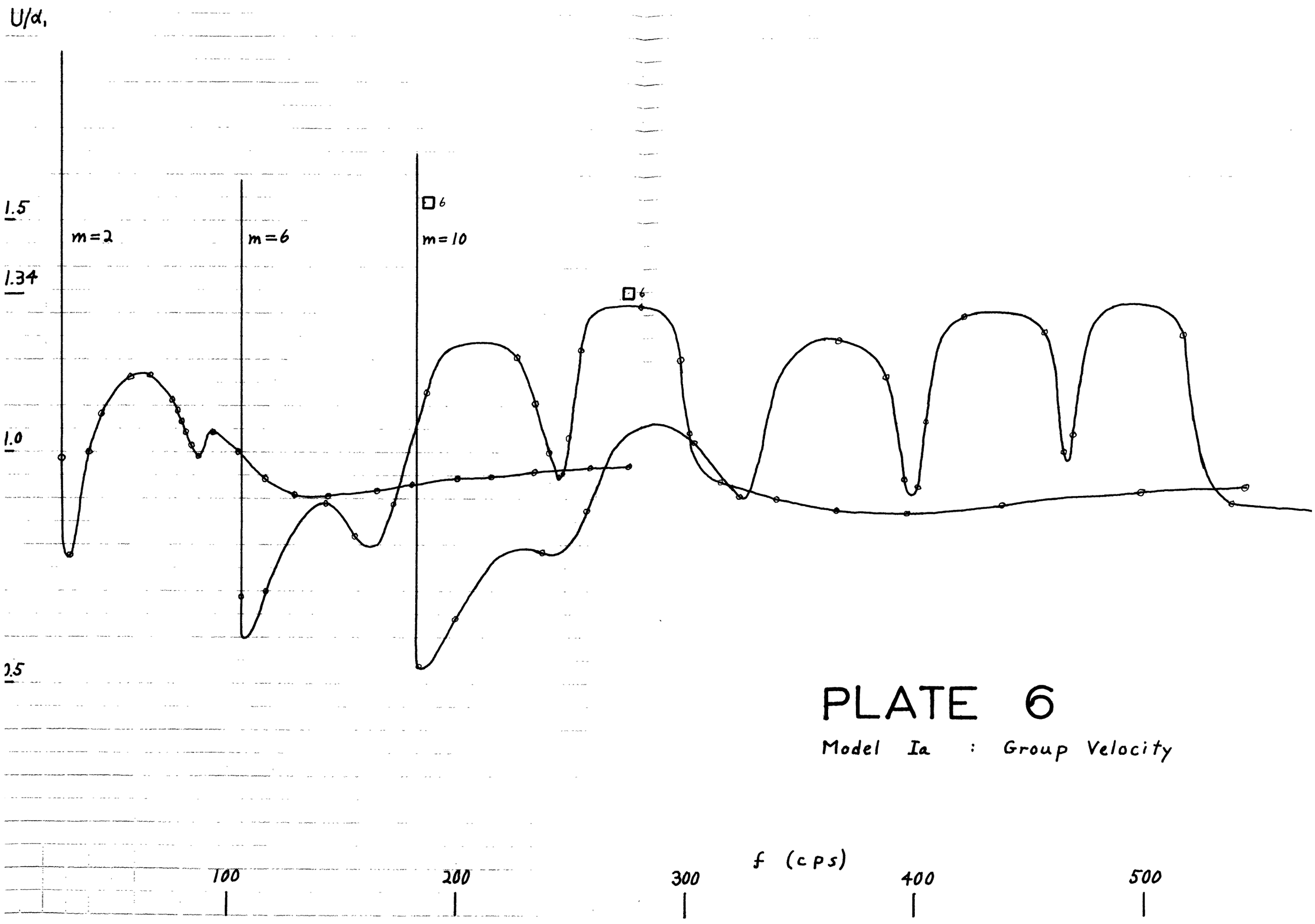

PLATE 6

Model Ia : Group Velocity

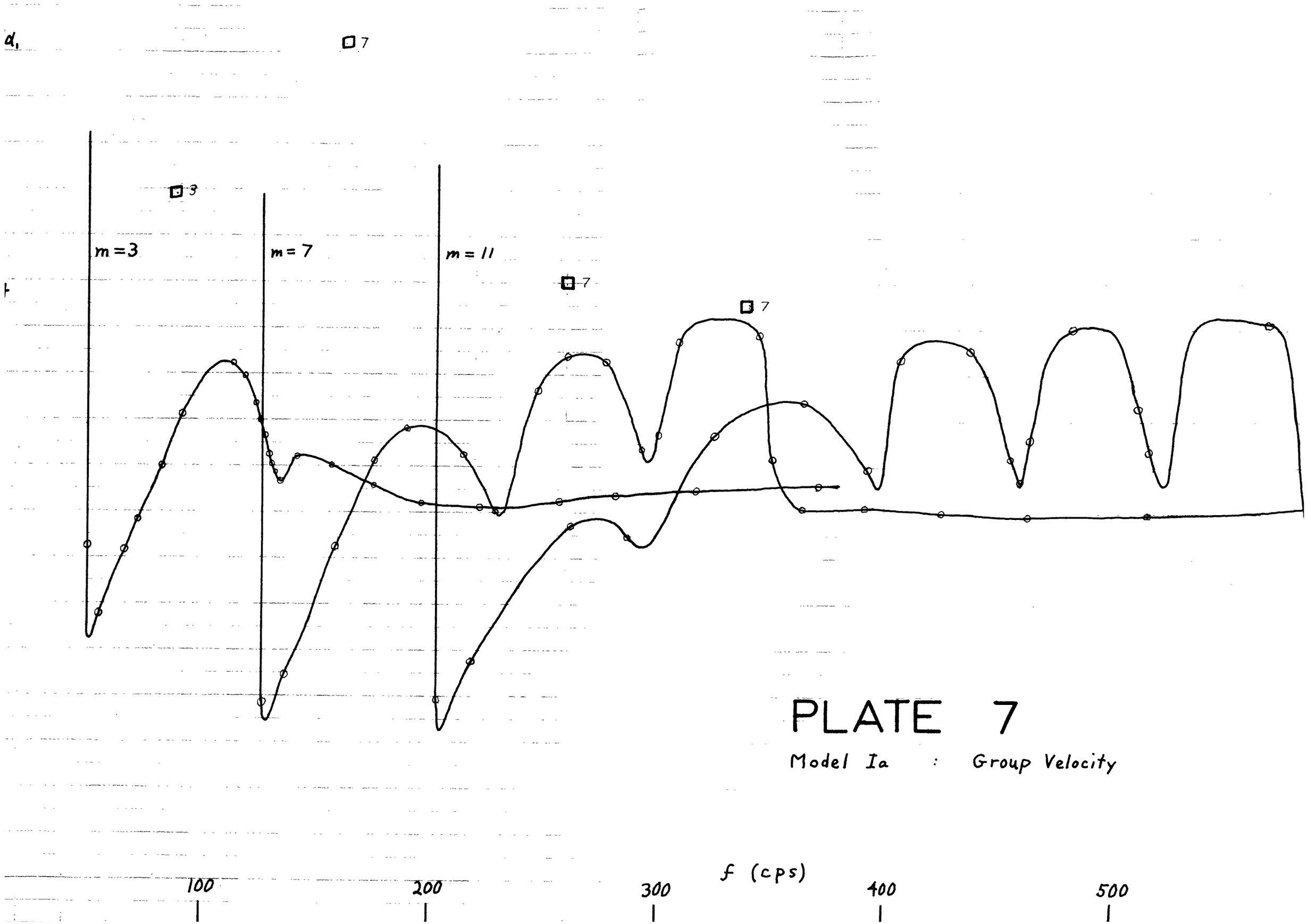

PLATE 7

Model Ia : Group Velocity

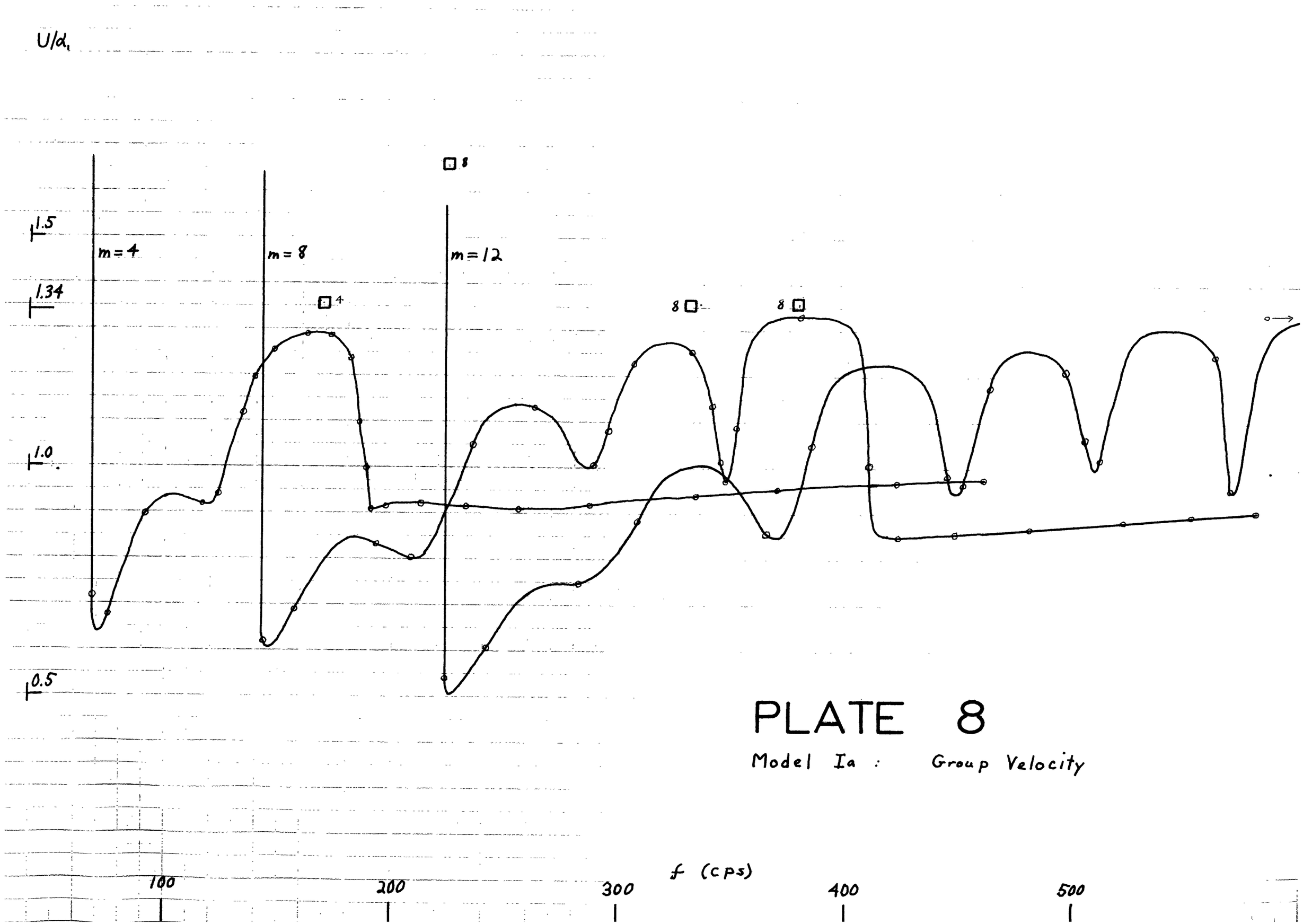

PLATE 8

Model Ia : Group Velocity

APPENDIX IV

LISTING OF 704 PROGRAM IN SAP LANGUAGE
MAY 18, 1959

```
        REM R.A. PHINNEY  SOLUTION OF FOUR LAYER ACOUSTIC PROBLEM
        ORG 1000
COMMON  BSS 50
 A      BSS 11
 KZ     BES 780
 GROUP  BES 780
 NZ     BES 720
 MD     BES 60
 ANS    BES 2450
 P      BSS 41
NA34.1  LIB                     SQUARE ROOT
UABDC1  LIB                     BINARY TO DECIMAL
UASTH1  LIB                     OUT PRINT ON LOGICAL 2
CLTAN1  LIB                     TANGENT
UADBC1  LIB                     INPUT DECIMAL TO BINARY
UACSH2  LIB                     ON LINE CARD READER) SS1 DOWN.
        REM INSERT INVERSE TANGENT DECK=  B1 UA ATN1

        REM END OF INVERSE TANGENT DECK=  B1 UA ATN1
        REM INSERT TANH DECK =  B2 BA F113

        REM END OF TANH DECK=  B2 BA F113
 AT     DEC 1.57079
 AU     DEC 3.14159,6.28318,9.42477,12.56636,15.70795,18.84954,21.99113
        DEC 25.13272,28.27431,31.41590,34.55749,37.69908
 AV     BSS 1
 GUTEN  DEC 60
 AJ     DEC 6283.18,.0001,1.,2.
 RECAP  PZE 720,0,779
 INDEX  PZE 60,0,12
        TSX LOAD,4
        PZE NZ,0,NZ+59
        TSX LOAD,4
        PZE A,0,A+10
        LXA INDEX,2
        REM BEGIN CALCULATION OF PARAMETERS DEPENDING ON THE MODEL
        LDQ A+1
        FMP A+1
        STO P
        LDQ A+2
        FMP A+2
        STO P+1
        LDQ A+3
        FMP A+3
        STO P+2
        CLA A+7
        FDP A+6
        STO P+3
        CLA A+6
```

```
        FDP A+5
        STQ P+4
        CLA A+5
        FDP A+4
        STQ P+5
        CLA A+8
        FDP A+10
        STQ P+6
        CLA A+9
        FDP A+10
        STQ P+7
        CLA A+8
        FDP A
        STQ P+9
        CLA A+9
        FDP A
        STQ P+10
        CLA A+10
        FDP A
        STQ P+11
        REM BEGIN CALCULATION OF PARAMETERS DEPENDING ON PHASE VELOCITY
PHASE   LXD INDEX,1
        LDQ MD,2
        FMP MD,2
        TZE CRAMR+1
        STQ P+12
        FDP P+2
        STQ P+13
        CLA AJ+2
        FSB P+13
        TSX SQRT,4
        NOP
        CHS                     TAG A4
        STQ P+12
        CLA P+12
        FDP P+1
        STQ P+14
        CLA P+14
        FSB AJ+2
        TMI LIMBO
        REM BEGINNING OF PAGE 4
        TSX SQRT,4
        NOP
        TRA GABRO
LIMBO   CHS
        TSX SQRT,4
        NOP
        CHS                     TAG A3
GABRO   STO P+14
        CLA P+12
        FDP P
        STQ P+15
        CLA P+15
        FSB AJ+2
        TMI LIMBS
        TSX SQRT,4
```

```
        NOP
        TRA GABRA
LIMBS   CHS
        TSX SQRT,4
        NOP
        CHS                     TAG A2
GABRA   STO P+15
        CLA P+12
        FSB AJ+2
        TSX SQRT,4
        NOP                     AUTOMATIC ERROR CHECK
        STO P+16
        LDQ AJ
        FMP P+11
        FDP MD,2
        REM BEGIN PAGE 5
        STQ P+17
        LDQ P+16
        FMP P+6
        STO P+18
        LDQ P+15
        FMP P+7
        STO P+19                Q TAGGED
        CLA P+14
        TPL SPECS               CHECK TAG OF A3
        CLA P+19
        TPL SOUPS
        TRA SLURP
SPECS   FAD P+19
SOUPS   FAD P+18
        TRA SLUMP
SLURP   CLA P+18
SLUMP   STO P+20
        FDP SLUMP+4
        STQ P+28
        TRA *+2
        DEC .25
        CLA A+6
        FDP P+14
        STQ P+21
        CLA P+21
        SSP
        FDP A+5
        FMP P+15
        STO P+21
        STZ P+23
        CLA A+5
        FDP P+15
        STO P+22
        CLA P+22
        SSP
        FDP A+4
        FMP P+16
        STO P+22
```

```
        CLA P+13
        TNZ CONF
        CLS AT
        TRA PAUL+2              PAUL+2 IS FAD
CONE    CLA A+7
        FDP P+13
        STQ P+23
        CLA P+23
        SSP
        FDP A+6
        FMP P+14
        STO P+23
HOBOB   TPL PAUL
        REM   LOOP IN NEW M
        CLA P+21                BEGIN CALCULATION OF EIGENVALUES
        TPL PAUL
        CLA P+22
PAUL    TSX ARTN,4
        CHS
        REM BEGINNING OF PAGE 7
        FAD AV,1
        FDP P+20
        REM LOOP IN NEW VALUE OF X
REPEA   STO P+30                LOOP IN X
        FMP P+14
        TMI ATTEN
        STO P+24
        CLA P+23
        TNZ *+3
        CLA AT
        TRA *+2
OPZ     TSX ARTN,4
        FAD P+24
        TRA RHINE
ATTEN   STO LODF
        TSX TNH,4               TANH SUBROUTINE
LODF    PZE 0,0,0               INPUT
        TRA DOLE                ERROR OUTPUT
        TRA ODEL                REGULAR OUPPUT
DOLE    CLS AJ+2
ODEL    STO P+35
        LDQ P+23
        FMP P+35
        FAD AJ+2
        STO P+36
        CLA P+35
        FSB P+23
        FDP P+36
        FMP P+21
        TPL *+4
        STZ P+32
        SXD P+33,1
        TRA NEIL
        SXD P+33,1
        STO P+35
        STZ P+32
```

```
        LDQ P+30
        REM BEGINNING OF PAGE 8
        FMP P+19
        STO LATE
        TSX TNH,4
LATE    PZE 0,0,0
        TRA TALE
        TRA TEAL
TALE    CLS AJ+2
TEAL    STO P+36
        LDQ P+35
        FMP P+36
        FSB AJ+2
        STO P+37
        CLA P+36
        FSB P+35
        FDP P+37                TANH(2)
        TRA LOUIE+2
RHINE   SXD P+33,1
        LXD INDEX,1
        REM BEGINNING OF PAGE 9
        FSB AT
        STO P+34
        STZ P+32
SUPER   TMI INVER
        FSB AV-12
        STO P+34
        CLA AV,1
        STO P+32
        CLA P+34
        TIX SUPER,1,1
        LXD P+33,1
        TRA CRAMR
INVER   FAD AT
        TSX TAN,4
        STO P+35
        LDQ P+35
        FMP P+21
        TRA DOWNS
NEIL    CHS
DOWNS   TSX ARTN,4
        FAD P+32                PROPER PHASX
        STO P+34
        LDQ P+30
        REM BEGINNING OF PAGE 10
        FMP P+19
        FAD P+34
        LXD INDEX,1         RESET INDEX FOR PHASE DETECTION USE
        FSB AT
        STO P+34
        STZ P+32
SUPET   TMI INVET
        FSB AV-12
        STO P+34
```

```
        CLA AV,1
        STO P+32
        CLA P+34
        TIX SUPET,1,1
        LXD P+33,1
        TRA CRAMR
INVET   FAD AT
        TSX TAN,4
LOUIE   STO P+34
        LDQ P+34
        FMP P+22
        TSX ARTN,4
        FAD P+32                TAN-1 OF LII WITH CORRECT PHASE
        STO P+34
        LDQ P+30
        REM BEGINNING OF PAGE 11
        FMP P+18
        FAD P+34                PSI SUB 1
        LXD P+33,1
        CHS
        FAD AV,1
        FDP P+28
        STQ P+34
        CLA P+34
        SSP
        CAS AJ+1
        TRA *+5
        NOP
        STZ P+36
        STZ P+37
        TRA *+6
        CLA P+34
        FAD P+30
        STO P+30
        LDQ P+30
        TRA REPEA+1
ALTER   SXD P+36,2              PREPARE IR4 FOR STORAGE FUNCTION
        SXD P+37,1
        LDQ GUTEN
        MPY P+37
        STQ P+35
        CLA P+35
        ADD P+36
        PDX 0,4                 SET UP IR4
        CLA P+30
        FDP P+11
        FMP MD,2
        FDP AU+1
        STQ KZ,4
HELP    LDQ P+17
        TLQ CRAMR
        TIX HOBOE,1,1           MODIFY M
        TRA CRAMR
HOBOE   TRA CONE-4
        REM BEGINNING OF PAGE 12
CRAMR   TIX PHASE,2,1           MODIFY C AND RETURN
```

```
       REM BEGIN CALCULATION OF GROUP VELOCITY
       LXA INDEX,2            USE IR2 TO COUNT C
       LXD RECAP,4            USE IR4 TO COUNT F AND U
CAPER  CLA KZ,4
       TZE ZERO
MUMPS  FSB KZ+1,4             DELTA F
       STO P+31
       CLA MD+1,2
       FSB MD+2,2             DELTA C
       FDP P+31
       STQ P+31
       CLA KZ,4
       FAD KZ+1,4
       FDP AJ+3
       FMP P+31               F DC/DF
       CHS
       FAD MD+2,2
       STO P+30
       LDQ MD+1,2
       FMP MD+2,2
       FDP P+30
       STQ GROUP,4
       TIX *+1,4,2
       TIX CAPER,2,2
ZERO   TNX CRUST,4,2
       TIX *+1,2,2
       CLA KZ,4
       TZE ZERO
       LXA INDEX,2
       TRA MUMPS
       REM BEGIN CALCULATION OF GAMMA
CRUST  LXA RECAP,1            BEGIN SUBROUTINE TO GENERATE GAMMA
CURSE  CLA A+8
       FAD A+9
       FAD A+10
       FDP A
       FMP K7-60,1
       STO NZ,1
       TIX CURSE,1,1
       REM  END OF MAIN PROGRAM
       REM END OF MAIN PROGRAM. COMMENCE RESHUFFLE AND PRINT OF ANSWERS
       TRA EGGS+1
       ORG 8202
GRAB   PZE 0,0,4
DRAG   PZE 0,0,1
RAGD   PZE 0,0,3
GRAD   PZE 2450,0,60
FELON  BSS 7
OAHU   DEC 60
EGGS   DEC 180
       LXD GRAB,4
       SXD FELON+6,4
       LXA GRAD,4
COOL   LXD GRAD,2
```

```
 POOL  LXD RAGD,1
       CLA MD,2
       STO ANS,4
       TNX END,4,1
 LOOP  SXD FELON,2
       SXD FELON+5,4
       LXD FELON+6,4
       PXD 0,4
       SUB DRAG
       STO FELON+1
       LDQ FELON+1
       MPY EGGS
       STO FELON+2
       PXD 0,1
       SUB DRAG
       STO FELON+3
       LDQ FELON+3
       REM  BEGINNING PAGE 2A
       MPY OAHU
       STQ FELON+3
       CLA FELON+3
       ADD FELON+2
       ADD FELON
       PDX 0,2
       LXD FELON+5,4
       CLA KZ-60,2
       STO ANS,4
       TNX END,4,1
       CLA NZ,2
       STO ANS,4
       TNX END,4,1
       CLA GROUP-60,2
       STO ANS,4
       TNX END,4,1
       LXD FELON,2
       TIX LOOP,1,1
       TIX POOL,2,1
       SXD FELON+5,4          STORE ANSWER INDEX
       LXD FELON+6,4          MODIFY BLOCK INDEX
       TNX END,4,1
       SXD FELON+6,4
       REM BEGINNING OF PAGE 3A
       LXD FELON+5,4          REPLACE ANSWER INDEX
       TRA COOL
 END   TSX INTER,4
       PZE ANS,0,ANS+2450
       TRA INDEX+3
FINISH HPR 63
 INTER TRA BLOCK              INTERLUDE INTO UABDC1
       BCD 9F9.4,F14.2,F9.4,F8.3,F14.2,F9.4,F8.3,F14.2,F9.4,F8.3
       END INDEX+1
```

Bibliography

1. Abeles, F.; Sur la propagation des ondes electromagnetiques dans les milieux stratifies. Ann. Phys. 3, p. 504-520, 1948.

2. Biot, M. A.; General theorems on the equivalence of group velocity and energy transport. Phys. Rev. 105, no. 4, p. 1129, 1957

3. Bunce, E.T., and Phinney, R. A.; Seismic refraction observations in Buzzards Bay, Massachusetts. Presented at 40th annual meeting of the American Geophysical Union, May 5, 1959, Washington, D.C. Paper in preparation.

4. Dorman, James; Theory and computation of properties of surface waves on layered media. Presented at 40th annual meeting of the American Geophysical Union, May 5, 1959, Washington, D. C.

5. Durschner, H.; Synthetic Seismograms from continuous velocity logs. Geophysical Prospecting, VI, No. 3, p. 272, Sept. 1958

6. Ewing, M.Crary, A. P., and Rutherford, H. M.; Geophysical investigations in the emerged and submerged Atlantic coastal plain, Part.I. Bull. Geol. Soc. Am., 48, p. 753-802, 1937.

7. Ewing, M., Jardetzky, W. S., and Press, F.; Elastic waves in Layered Media. McGraw-Hill, New York, 1957.

8. Ewing, M., and Press, F.; Low speed layer in water covered areas. Geophysics, XIII, No. 3, p. 404, July 1948.

9. Ewing, M. Woollard, G. P., and Vine, A. C.; Geophysical investigations in the emerged and submerged Atlantic coastal plain, Part III.

10. Ibid, Part IV. Bull. Geol. Soc. Am., 51, p. 1821-1840, 1940.

11. Jardetzky, W. S.; Period equation for an n-layered halfspace. Lamont Geological Observatory Technical Report, Seismology, 29, 1953.

12. Levin, F. K., and Hibbard, H. C.; Three dimensional model studies. Geophysics, XX, No. 1, p. 19-32, Jan. 1955.

13. Officer, C. B. Jr.; An Introduction to the Theory of Sound Transmission, McGraw-Hill, New York, 1958.

14. Officer, C. B. Jr.; Normal mode propagation in a three-layered liquid halfspace by ray theory. Geophysics, XVI, No. 2, p. 207, April, 1951.

15. Pekeris, C. L.; Theory of propagation of explosive sound in shallow water. from G. S. A. Memoir No. 27: Propagation of Sound in the Ocean; Oct. 1948.

16. Press, Frank; Remarks on refraction arrivals from a layer of finite thickness. Presented at the Conference on Elastic Wave Propagation, California Institute of Technology, March 7-8, 1957; Journal of Geophysical Research, 63, No. 3, p. 631-634, Sept. 1958.

17. Sato, Y; Numerical integration of the equation of motion for surface waves in a medium with arbitrary variation of material constants. Bulletin of the Seismological Society of America, 49, p. 57-77, Jan. 1959.

18. Schelkunoff, S. A.; Remarks concerning wave propagation in stratified media. Commun. Pure and Applied Math., IV, No. 1, 117-128, 1951.

19. Tatel, H. E., and Tuve, M. A.; Seismic exploration of a continental crust. G. S. A. Special Paper No. 62, p. 35-50, 1955.

20. Tolstoy, I. and Usdin, E.; Dispersive properties of stratified elastic and liquid media: A ray theory. Geophysics, XVIII, No. 4, P.844, Oct. 1953.

21. Tolstoy, I.; Note on the propagation of normal modes in inhomogeneous media. Journal of the Acoustical Society, 27, p. 274, 1955.

22. Ibid; Dispersion and simple harmonic point sources in wave ducts. J. Acoust. Soc., 27, No. 5, p. 897, 1955.

23. Ibid; Resonant Frequencies and high modes in layered waveguides. J. Acoust. Soc., 28, No. 6, p. 1182, 1956.

24. Ibid; Shallow water test of the theory of layered waveguides. J. Acoust. Soc., 30, No. 4, P. 348, 1958.

25. Worzel, J. L., and Ewing, M.; Explosion sounds in shallow water. from G. S. A. Memoir No. 27; Propagation of Sound in the Ocean. Oct. 1948.